Accepted Manuscript

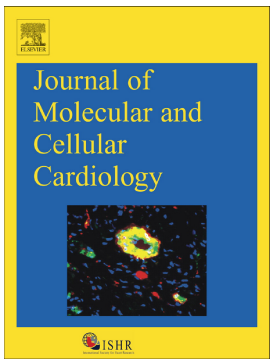

Role of neutrophils in CVB3 infection and viral myocarditis

Leonardo Rivadeneyra, Nancy Charo, Denise Kviatcovsky, Silvia de la Barrera, Ricardo Martín Gómez, Mirta Schattner

PII: S0022-2828(18)30717-X
DOI: doi:10.1016/j.yjmcc.2018.08.029
Reference: YJMCC 8838

To appear in: *Journal of Molecular and Cellular Cardiology*

Received date: 26 July 2018
Accepted date: 5 August 2018

Please cite this article as: Leonardo Rivadeneyra, Nancy Charo, Denise Kviatcovsky, Silvia de la Barrera, Ricardo Martín Gómez, Mirta Schattner , Role of neutrophils in CVB3 infection and viral myocarditis. Yjmcc (2018), doi:10.1016/j.yjmcc.2018.08.029

This is a PDF file of an unedited manuscript that has been accepted for publication. As a service to our customers we are providing this early version of the manuscript. The manuscript will undergo copyediting, typesetting, and review of the resulting proof before it is published in its final form. Please note that during the production process errors may be discovered which could affect the content, and all legal disclaimers that apply to the journal pertain.

ACCEPTED MANUSCRIPT

Role of neutrophils in CVB3 infection and viral myocarditis

Leonardo Rivadeneyra[a#&], Nancy Charo[a#], Denise Kviatcovsky[b], Silvia de la Barrera[b], Ricardo Martín Gómez[c*] and Mirta Schattner[a*]

a. Laboratory of Experimental Thrombosis, Institute of Experimental Medicine-CONICET-ANM, Buenos Aires, Argentina.

b. Laboratory of Immunology of Respiratory Diseases, Institute of Experimental Medicine-CONICET-ANM, Buenos Aires, Argentina.

c. Biotechnology and Molecular Biology Institute, CONICET-UNLP, La Plata, Argentina.

#both authors contributed equally

*both authors jointly designed and supervised the study and are the corresponding authors.

&Present Address: Blood Research Institute, BloodCenter Wisconsin
8727 W. Watertown Plank Rd, Milwaukee, WI 53226

Leonardo.Rivadeneyra@BCW.edu

nancycharo@hotmail.com

denise.kv@hotmail.com

sdelab@hematologia.anm.edu.ar

Corresponding Authors:

RMG: IBBM, CONICET-UNLP, Calle 49 y 115, 1900 La Plata. Argentina, Tel:+542216977
rmg1426@gmail.com

MS: IMEX, CONICET-ANM, Pacheco de Melo 3081, Buenos Aires, Argentina, Tel+:541148073926,
mschattner@hematologia.anm.edu.ar

ACCEPTED MANUSCRIPT

Abstract

Coxsackievirus B3 (CVB3) is a globally prevalent enterovirus of the *Picornaviridae* family that is frequently associated with viral myocarditis (VM). Neutrophils, as first responders, may be key cells in determining viral disease outcomes; however, neutrophils have been poorly studied with respect to viral infection. Although neutrophils have been ascribed a relevant role in early cardiac inflammation, their precise role in CVB3 infection has not yet been evaluated. In this study, we aimed to determine if the interaction between human neutrophils and CVB3 could lead to viral replication and/or modulation of neutrophil survival and biological functions, and whether neutrophil depletion in a murine model has a beneficial or harmful effect on CVB3 infection. Our results show that CVB3 interacted with but did not replicate in human neutrophils. Neutrophils recognized CVB3 mainly through endosomal TLR-8, and infection triggered NFκB activation. Virus internalization resulted in increased cell survival, up-regulation of CD11b, enhanced adhesion to fibrinogen and fibronectin, and the secretion of IL-6, IL-1β, TNF-α, and IL-8. Supernatants from infected neutrophils exerted chemotactic activity partly mediated by IL-8. The infected neutrophils released myeloperoxidase and triggered neutrophil extracellular trap formation in the presence of TNF-α. In mice infected with CVB3, viral RNA was detected in neutrophils as well as in mononuclear cells. After neutrophil depletion, mice showed reduced VM reflected by a reduction in viral titers, cell exudates, and CCL-2 mRNA levels, as well as the abrogation of reactive cardiomyocyte hypertrophy. Our results indicate that neutrophils have relevant direct and indirect roles in the pathogenesis of CVB3-induced VM.

Keywords: neutrophils, CVB3, myocarditis, inflammation, enterovirus

ACCEPTED MANUSCRIPT

Abbreviations: CVB3, Coxsackievirus B3; FBS, fetal bovine serum; EeF1A, eukaryotic translation elongation factor 1A; ECM, extracellular matrix; HNE, human neutrophil elastase; HSV-1, herpes simplex virus 1; IAV, influenza A virus; MOI, multiplicity of infection; MPO, myeloperoxidase; NETs, neutrophil extracellular traps; PFU, plaque forming units; ROS, reactive oxygen species; TLR, Toll-like receptor; VM, viral myocarditis; VP1, viral protein 1.

ACCEPTED MANUSCRIPT

ACCEPTED MANUSCRIPT

1. Introduction

CVB3 is a globally prevalent enterovirus of the *Picornaviridae* family [1] that is frequently associated with viral myocarditis (VM) [2]. While acute VM is typically self-limiting in most individuals, the development of severe heart muscle injury and/or its persistence, sustained by post-viral immune-mediated responses, may lead to dilated cardiomyopathy and heart failure in some [3]. The mechanisms underlying the pathogenesis of VM are not well-established. Furthermore, therapies for VM are not specific and are directed toward supportive care for heart failure [4]. The last stage of inflammatory heart disease, resulting in heart failure with transplantation as a frequent therapeutic option, is a major healthcare burden worldwide [3].

The CVB3 murine model has provided significant insights into the pathogenesis of VM, as it shares many biological parameters of acute and chronic CVB3-induced diseases in humans [2, 5]. A direct role for virus replication, as well as several immune-mediated mechanisms, have been involved in CVB3-induced VM [2, 5].

In humans, neutrophils are the most abundant subset of leukocytes, and they play a crucial role in host responses against invading pathogens through an arsenal of toxic molecules stored in their intracellular granules, which are released upon activation or fused with intracellular compartments containing phagocytosed microbes. In addition, neutrophils can produce reactive oxygen species (ROS) through NADPH activation and synthesize cytokines with pro-inflammatory activity. Neutrophils are also able to neutralize microbes through the release of neutrophil extracellular traps (NETs) [6].

In the acute phase of CVB3-induced VM in mice, early cardiac innate cell infiltration consisting of macrophages, neutrophils, NK cells and γδ T cells has been demonstrated [7]. Although neutrophils have been ascribed to play a relevant role in early cardiac inflammation [8, 9], their precise role in CVB3 infection has not yet been studied.

ACCEPTED MANUSCRIPT

Therefore, we aimed to determine if the interaction between human neutrophils and CVB3 could lead to viral replication and the modulation of neutrophil biological functions. In addition, we studied whether depletion of neutrophils would have a beneficial or harmful effect on CVB3-induced murine VM.

2. Materials and methods

2.1 Isolation of neutrophils

This study was performed according to institutional guidelines (National Academy of Medicine, Buenos Aires, Argentina) and was approved by the Institutional Ethics Committee. All subjects provided written informed consent for sample collection and subsequent analysis.

Neutrophils were isolated from peripheral blood drawn from healthy donors. Briefly, blood samples were centrifuged on a Ficoll-Hypaque gradient (1.078 g/ml density, GE Healthcare, Buckinghamshire, UK) at 400 x *g* for 30 min at room temperature (RT) followed by 6% dextran sedimentation (Sigma, MO, USA) and hypotonic lysis of erythrocytes [10]. Cell suspensions that contained ≥99.5% neutrophils as determined by flow cytometry were used in all experiments. Neutrophils were suspended in RPMI 1640 supplemented with 2% fetal bovine serum (FBS) (GIBCO, NY, USA). In selected experiments, neutrophils or mononuclear cells (obtained after the Ficoll-Hypaque gradient) were stimulated with CL264 or TL8-506 (InvivoGen, CA, USA) (TLR-7 and TLR-8 agonists, respectively) or treated with bafilomycin A1 (inhibitor of the vacuolar type H^+ATPase) (InvivoGen).

2.2 Cells and viral stocks

Vero-76 cells (American Type Culture Collection, VA, USA) were maintained as monolayers in RPMI 1640 (GIBCO) supplemented with 10% FBS. The myocarditic CVB3

ACCEPTED MANUSCRIPT

(H3) strain [11] was propagated in Vero cells, and infectivity titration assays were performed as previously described [12].

2.3 Cell infection

Neutrophils ($1x10^5$) or a monolayer of Vero cells ($1x10^5$) (as a positive control) were inoculated with CVB3 at a multiplicity of infection (MOI) of 0.1, 1 and 10 for 3 h at 37ºC. After three exhaustive washes to ensure viral removal, neutrophils and Vero cells were suspended in 200 µl of RPMI 1640 with 2% FBS. Mock infection (as a negative control) was performed by replacing the same volume of virus inoculum with uninfected Vero cell supernatant.

2.4 Viral detection by immunofluorescence and flow cytometry

Neutrophils ($1x10^5$) or a monolayer of Vero cells ($1x10^5$) were incubated with CVB3 (MOI of 1) for 3 h, washed and cultured for 1 and 24 h post-infection (hpi) in RPMI medium supplemented with 2% FBS. At any given time point, cells were fixed with 1% paraformaldehyde (PFA), centrifuged and permeabilized with 0.1% Triton X-100. After blocking with 10% FBS, the cells were incubated for 1 h with the primary antibody (Ab) against the enterovirus VP1 capsid protein (Dako, Glostrup, Denmark), followed by an Alexa Fluor 488-conjugated secondary Ab (Life Technologies, NY, USA). Cells were mounted on slides and analyzed by confocal microscopy (Olympus FV-1000, Tokyo, Japan). Surface and intracellular detection of CVB3 were determined by flow cytometry in non-permeabilized or permeabilized neutrophils, respectively. After infection, the cells were centrifuged and treated for 30 min with Fix and Perm (BD Biosciences, CA, USA) and after washing and blocking with 10% FBS, incubated for 1 h with VP1 Ab. Thereafter,

ACCEPTED MANUSCRIPT

the cells were stained with an Alexa Fluor 488-conjugated secondary Ab for further 15 min and finally suspended in Isoflow (BD) and analyzed using a FACSCalibur flow cytometer (BD Biosciences) by acquiring 10,000 events in the neutrophil gate.

2.5 RT-PCR and qPCR

The presence of viral RNA, as well as TLR-7, TLR-8, CCL-2 and Eef1A mRNA was analyzed by RT-PCR/qPCR using specific primers (5'>3'): CVB3 fwd: CGGCCCCTGAATGCGGCTAA, rev: GAAACA CGGACACCCAAAGTA; TLR-7 fwd: CAAGAAAGTTGATGCTATTGGGC, rev: TTCGTGGTGTTCGTGGGAAT; TLR-8 fwd: AGAACA-ACAGAAACATGGAAAACAT, rev: CCGTTTGGGGAACTTCCTGT; CCL-2 fwd: TGCCCTAAGGTCTTCAGCAC, rev: AAGGCATCACAGTCCGAGTC; Eef1A fwd: TCGGGCAAGTCCACCACTAC, rev: CCAAGACCCAGGCATACTTGA. Total RNA was isolated from cell or tissue pellets using TriReagent (Genbiotech, BsAs, Argentina). Prior to cDNA synthesis, DNase treatment was performed with an RNase-free DNase Kit (Qiagen, CA, USA). The cDNA was synthesized from 1 µg of total RNA using 15 mM of random hexamers (Biodynamics, BsAs, Argentina) and MMLV reverse transcriptase (Promega, BsAs, Argentina). The obtained cDNA was used as a template for PCR, with the experiments performed in triplicate. For CCL-2, the qPCR procedure was used as previously described [13].

2.6 Detection of neutrophil supernatant infectivity by viral plaque assays

To determine whether neutrophils were infected, the cells ($1x10^5$) were incubated with CVB3 at an MOI of 1 for 3 h. Vero cells were then incubated with supernatants or pellets from CVB3-treated neutrophils and cultured in a medium with methylcellulose for 72 h. The

ACCEPTED MANUSCRIPT

formation of plaque forming units (PFU) was revealed by methanol and crystal violet staining [12].

2.7 Expression of CD11b

To evaluate CD11b expression, neutrophils ($1x10^5$) were infected with CVB3 and then at different times pi, the cells were fixed and stained with PE-conjugated CD11b or an irrelevant IgG1 (Biolegend, CA, USA). The cells were then analyzed by flow cytometry.

2.8 Neutrophil adhesion assay

A 96-well plate was coated with fibrinogen (100 µg/ml) or fibronectin (10 µg/ml) and left overnight at 4°C. The plate was then washed and blocked with 2% heat-inactivated BSA, and aliquots of neutrophils ($1x10^5$) were added to each well, uninfected or infected with CVB3, and then incubated at 37ºC for 3 h. After washing, a solution of 5 mM p-nitrophenyl phosphate in 0.1 M citrate buffer containing 0.1% Triton X-100, pH 5.4 was added and incubated for 1 h at 37ºC. The reaction was stopped by adding 2 N NaOH, and the absorbance at 405 nm was measured with a microplate reader (Dynatech MR 5000; Dynatech Laboratories).

2.9 Production of pro-inflammatory cytokines and IL-8

After neutrophil infection with CVB3 for 18 h, the cells were centrifuged at 600 x *g* for 10 min and the production of IL-6, IL-1β, TNF-α and IL-8 was determined in the supernatants with commercial ELISA kits (eBioscience, CA, USA) used according to the manufacturer's instructions.

ACCEPTED MANUSCRIPT

2.10 Neutrophil chemotaxis assay

Neutrophils ($1x10^5$) were suspended in RPMI with 2% FBS, and chemotaxis was quantified using a modification of the Boyden chamber technique. Cell suspension was placed in the upper wells of an 18-well micro chemotaxis chamber (Neuro Probe, MD, USA), separated by a polyvinylpyrrolidone (PVP)-free polycarbonate filter (3 µm pore size; Poretics Products, CA, USA). The lower wells contained the supernatant from infected or uninfected neutrophils. The chamber was incubated for 30 min at 37°C in a 5% CO_2 humidified atmosphere. Following incubation, the chamber was disassembled and the membrane removed, fixed and stained with Staining 15 (Biopur Diagnostics, Argentina). The number of neutrophils that migrated through the filter was counted in five random high-power fields at a magnification of 400x per condition (each condition in triplicate) employing an optical microscope. Results are expressed as the number of migrated neutrophils per field. In selected experiments, supernatants from infected neutrophils were incubated with a neutralizing Ab against IL-8 or an IgG control.

2.11 Determination of neutrophil apoptosis and viability

Neutrophils were cultured in RPMI with 2% FBS in the presence or absence of CVB3. At 24 hpi, the cells were analyzed for changes in nuclear morphology and viability by labelling with a mixture of acridine orange and ethidium bromide (100 µg/ml) to determine the percentage of cells that had undergone apoptosis [14]. Apoptosis was also determined by analyzing the percentage of hypodiploid cells. After infection, the cells were fixed with ice-cold 70% ethanol overnight, washed three times, and then suspended in a solution containing 1 mg/ml RNase and 2 µg/ml propidium iodide (PI) (Sigma). After 15 min, the cells were analyzed by flow cytometry.

2.12 Immunoblotting

ACCEPTED MANUSCRIPT

Neutrophils were incubated for 3 h with CVB3 and then solubilized in loading buffer (62.5 mM of Tris-HCl at pH 6.8, 25% glycerol, 2% SDS, 0.01% bromophenol blue and 5% 2-mercaptoethanol). Equal amounts of sample proteins were electrophoresed on a 10% SDS-PAGE gel and electrotransferred to nitrocellulose membranes. After blocking, the membranes were incubated with primary Abs anti-IκBα and anti-β-actin (BD Biosciences), followed by incubation with HRP-conjugated secondary Abs. Protein bands were visualized by enhanced chemiluminescence (ECL Plus; GE Healthcare, Buckinghamshire, UK).

2.13 Myeloperoxidase activity

Myeloperoxidase (MPO) activity was measured in supernatants from neutrophils uninfected or infected with CVB3 for 3 h at 37°C in RPMI 1640 medium supplemented with 2% FBS. MPO was evaluated by adding the high sensitivity substrate TMB (Thermo Fisher Scientific, MA, USA), and absorbance was read at 450 nm after stopping the reaction with 2 N sulfuric acid. The calibration curve was constructed using purified MPO of a known concentration.

2.14 Generation of reactive oxygen species

To determine reactive oxygen species (ROS) production, uninfected or infected neutrophils were incubated with dihydrorhodamine (DHR, 5 μM) for 30 min at 37°C and analyzed by flow cytometry.

2.15 Formation of neutrophil extracellular traps (NETs) and DNA release quantification

Neutrophils ($1x10^5$) were seeded in 24-well flat-bottom-plates with coverslips, infected with CVB3 and with or without TNF-α (10 ng/ml) and placed in a humidified incubator at 37°C

ACCEPTED MANUSCRIPT

with CO_2 (5%) for 180 min. The cells were then fixed with PFA (1%), blocked with 10% heat-inactivated FBS and stained with rabbit anti-human elastase (HNE) or the corresponding IgG controls (Calbiochem-Merck Millipore, Darmstadt, Germany). For HNE identification, cells were incubated with an Alexa Fluor 488-labeled goat anti-rabbit secondary Ab and the DNA was stained with PI (20 µg/ml). Mounted specimens were analyzed by confocal fluorescence microscopy. For quantification purposes, neutrophils were incubated with CVB3 or TNF-α (10 ng/ml) plus CVB3 (MOI=1) in the absence or presence of bafilomycin A1 (50 nM), Then, DNA released from neutrophils during NETosis was digested with micrococcal nuclease (500 mU/ml, Roche Diagnostics, Mannheim, Germany) for 15 min. EDTA (5 mM) was added to stop the nuclease activity, and the supernatants were collected and centrifuged, after which the DNA was measured using SYBR Gold in a fluorometer (BioTek Instruments, VT, USA). TL8 506 was used as a TLR-8 agonist. The calibration standard curve was constructed using thymus DNA of a known concentration [15].

2.16 Neutrophil depletion and mouse infection

All experiments were performed in accordance with the American Physiological Society's Guiding Principles for the Care and Use of Animals in Research (American Physiological Society) and federal law on the use of experimental animals (Animal Welfare Act) and were approved by the Institutional Animal Care and Use Committee.

Male C57BL/6 mice, 6 to 7 weeks old (Charles River Laboratories, Wilmington, MA), were housed in a level 2 containment facility. Food and water were available *ad libitum.* The conditions of the mice were monitored daily. Neutrophil depletion was induced by an intraperitoneal (i.p.) inoculation with 100 µl of PBS (endotoxin-free) containing 100 µg of anti-Ly6G (1A8clone, BioXCell, NH, ref BE0075-1) every 24 h. Control mice were inoculated with an isotype control Ab (clone 2A3, BioXCell, ref BE0089) under the same

ACCEPTED MANUSCRIPT

conditions. The first inoculation was performed one day before infection and then at every 24 h. Mice were i.p. inoculated with $2x10^5$ PFU of virus in 200 µl of PBS. To determine viremia, on 2 dpi, the mice were anesthetized with an i.p. injection of 2,2,2-tribromoethanol in tert-amyl alcohol (Avertin; Aldrich Chemical Co., WI, USA) and blood was drawn into plastic tubes containing 3.8% sodium citrate. The plasma sample was obtained by centrifugation at 600 x *g* for 10 min. On day 7 pi, all mice were anesthetized with Avertin, and blood samples were obtained to determine hematological counts using a veterinary hematological analyzer (Abacus Jr Vet, Vienna, Austria). Afterward, the mice were euthanized by cervical dislocation, and the hearts were removed aseptically and split in half along the long axis. One part was homogenized using a Bio-Gen PRO200 homogenizer, as recommended by the manufacturer, in 1 ml of sterile PBS. After clarification, the homogenates were titrated for virus infectivity determination. The other half was fixed in 4% PFA, processed for routine histology and used to determine a myocarditis score [13].

2.17 Immunohistochemistry

Cell exudates were characterized as previously described with minor modifications [13, 16] using 8-µm paraffin-embedded sections from the CVB3, Iso + CVB3 and 1A8 + CVB3 groups since there were no infiltrates in the control and 1A8 groups. In contrast, for p53 expression studies, all groups were included. Briefly, after rehydration, the tissue Pro-Bond Plus sections were heated three times for 5 min in 10 mM citrate buffer in a microwave oven. The sections were then cooled and immersed in 3% H_2O_2 for 15 min to inhibit endogenous peroxidase activity. To block non-specific antigen sites, sections were incubated with PBS + 5% normal goat serum for 20 min at RT. Sections were then incubated with the respective primary antibodies: anti-CD4, anti-CD8, anti-CD45R and anti-p53 (Immunotools, Germany). In addition, we used anti-neutrophil (clone 1A8) and

ACCEPTED MANUSCRIPT

anti-macrophage (MAC-2, clone M3/38) antibodies. The primary antisera were applied to sections overnight at 4°C, washed for 15 min, and then incubated with the secondary Ab (goat anti-rabbit/mice immunoglobulin) conjugated to peroxide-labeled dextran polymer (DAKO EnVision) or anti-rat peroxidase for 20 min at RT and again washed with PBS. Diaminobenzidine/hydrogen peroxidase substrate (DAB) was added until the appropriate intensity was obtained and slides were then rinsed with distilled water to stop the staining reaction. Immunostained sections were slightly counterstained with hematoxylin and dehydrated, mounted and observed under a Nikon E200 photomicroscope. As a control for the effectiveness of the primary Ab, sections were equally treated but without primary Ab incubation. Quantification of the cells in infiltrates was performed by counting immunostained cells, using a 40x objective with a grid area of 0.04 mm^2. Serial sections were made from areas with inflammation and/or necrosis in order to analyze the same area with different antibodies. Three animals were examined for each condition. Ten to twenty grids from each section were evaluated. The total number of infiltrating cells counted was generally about 100-200.

2.18 Analysis of cardiomyocyte size

Samples used for analysis were taken from formalin-fixed paraffin embedded hearts from all groups of mice studied. After rehydration, samples were stained with HBSS containing Alexa Fluor 594-conjugated wheat germ agglutinin (WGA, 5 μg/ml, Invitrogen, Argentina) to delineate the cell membrane [17]. Samples were washed and mounted in a solution containing DAPI for nuclear staining and photographed in a Nikon E200 equipped with a fluorescence system. For the analysis of cardiomyocyte size, Image J software (NIH, USA) was used following the instructions provided with the software and whole-slide images were sampled to a final resolution of 1.0 μm/pixel. Only cells with well-defined cell

ACCEPTED MANUSCRIPT

membranes and visible cell nuclei at mid-wall depth with an apparent transversal orientation were selected. At least 100 cells were counted for each sample.

2.19 Isolation of neutrophils from murine white blood cells by fluorescence activated cell sorting (FACS).

Briefly, infected C57BL/6 mice were anesthetized with Avertin and bled at 2 days post-infection. Whole blood samples were centrifuged at 600 x g for 15 min at RT and the platelet-rich plasma was discarded. After the lysis of murine red blood cells, leukocytes were blocked with physiological saline solution + 5% FBS and then were stained with anti-VP1 and Ly6G Abs, followed by conjugated secondary Abs. Cells were then resuspended in Isoflow (BD) and analyzed by flow cytometry by acquiring 10,000 events in the neutrophil gate. To sort the population of pure neutrophils (Ly6G+ cells), the same procedure described above was followed, but cells were only stained with Ly6G Ab. Sorting was performed with a FACS Aria fusion apparatus. A post-sort analysis was performed to determine the purity of neutrophils, which was 98.2±0.4%.

2.20 Statistical analysis

The results are expressed as the mean and the SEM. Each n represents a different donor. One-way analysis of variance (ANOVA), followed by the Bonferroni test, was employed to determine the significance of differences between groups. A *P* value lower than 0.05 was considered to be statistically significant.

3. Results

ACCEPTED MANUSCRIPT

3.1 CVB3 is internalized by neutrophils

We initially explored the CVB3-neutrophil interaction by incubating human neutrophils with CVB3 at several time points, followed by immunofluorescent detection of viral antigen. Extensive washing was performed prior to virus detection to ensure removal of the exogenously inoculated virus, and infected Vero cells were used as positive controls. The CVB3 VP1 capsid protein was detected by immunofluorescence in some neutrophils at 1 and 24 hpi, as well as in the Vero cells (1 hpi) used as positive controls (Figure 1A). To address whether the virus was located in the membrane or in the intracellular compartment, flow cytometry experiments were performed in both permeabilized and non-permeabilized cells. In non-permeabilized infected neutrophils, the percentage of cells containing surface-associated viral antigen was 4%±1, while this value increased to 11±2% (n=3) in permeabilized cells, indicating that CVB3 was mostly internalized by neutrophils (Figure 1B).

3.2 CVB3 does not replicate in neutrophils

Given that CVB3 was detected in human neutrophils, we wondered whether the virus was able to replicate in these cells. For that purpose, the infectivity titers in pellets or supernatants were determined over time. Although infectious CVB3 was detected in both neutrophil supernatants and pellets, the viral titer levels diminished with time (Figure 2A). In contrast, and as expected, the Vero-infected supernatants and pellets showed a significant increase in infectivity titer levels from 1 to 24 hpi (Figure 2A), with almost 100% of the monolayer showing a cytopathic effect at 24 hpi.

Considering the short half-life of neutrophils and that the lack of increasing titers may be due to increasing cell death, we explored if the negative-sense single stranded RNA, theoretically present only in cells with ongoing viral genome replication, could be detected. Unexpectedly, the results showed not only the negative strand in the infected cells but also

ACCEPTED MANUSCRIPT

in the viral stock (Supplementary Figure 1). To further determine if the virus replicated in neutrophils, the levels of viral RNA versus time were analyzed by semi-quantitative RT-PCR. The results show that the viral RNA in neutrophils clearly diminished over time (Figure 2B). Together, these data strongly suggest that CVB3, although incorporated into the neutrophil cytoplasm, does not replicate.

3.3 CVB3 increases neutrophil binding to ECM and chemokine release

As it has been demonstrated that some viruses induce several neutrophil activation responses, including CD11b expression [18], the main mediator of neutrophil-endothelial cell interaction, we next explored CD11b expression on CVB3-infected neutrophils. Figure 3A shows that CVB3 infection resulted in increased CD11b expression levels after 1 hpi, in an MOI-dependent manner. Because CD11b is a receptor with several ligands, including many proteins associated with the extracellular matrix (ECM) [19, 20], the eventual functionality of its increased expression was analyzed by studying neutrophil adhesion to plates coated with fibrinogen or fibronectin at 3 hpi (followed by phosphatase acid activity quantification). While non-infected neutrophils showed little adhesion to either fibrinogen or fibronectin, neutrophils infected with CVB3 had an enhanced ability to bind to both ECM proteins (Figure 3B and Supplementary Figure 2A). Because IL-8 is a major chemokine known to facilitate neutrophil extravasation [21], in the next experiments, we studied if CVB3 infection induced IL-8 secretion. Figure 3C shows that the levels of IL-8 in the supernatants from infected neutrophils were significantly higher than those observed in non-infected or mock samples. As human circulating neutrophils enter the site of infection by mainly migrating along a gradient of IL-8, and to find a functional correlate of this IL-8 increase, the chemoattractant capacity of the supernatants derived from infected and non-infected cells was evaluated using a modified Boyden chamber assay. While supernatants from mock samples exerted a slight but significantly higher chemoattractant activity

ACCEPTED MANUSCRIPT

compared with control samples, supernatants derived from CVB3-infected neutrophils showed a significantly higher ability to attract neutrophils than those from mock and non-infected cells (Figure 3D and Supplementary Figure 2B). Preincubation of supernatants from CVB3-infected neutrophils with a neutralizing Ab against IL-8 significantly diminished chemotaxis, suggesting a relevant role of this chemokine in the chemoattractant activity of neutrophils (Figure 3D).

3.4 CVB3 infection increases neutrophil survival

Because exposure to bacteria is known to prolong neutrophil half-life through the inhibition of apoptosis [22], we explored whether CVB3 had a similar effect. At 24 hpi, analysis of the nuclear morphology showed that CVB3 infection induced a reduction in the number of apoptotic cells (Figure 4A). In addition, flow cytometric studies also showed that the number of hypodiploid cells was significantly lower in infected cells compared with mock and control neutrophils (Figure 4B). To determine whether the increase in cell survival was associated with the secretion of cytokines, we evaluated the levels of several cytokines known to modulate the neutrophil fate. CVB3 infection induced a significant increase in the levels of IL-1β, TNF-α and IL-6 (Figure 4C). Moreover, in order to determine whether infectious virus was required to induce cytokine release, neutrophils were exposed to UV-inactivated CVB3. We found no differences in the release of IL-6 induced by infective or non-infective CVB3 (Figure 4C).

Activation of the transcription factor NFκB is a major pathway involved in cytokine release upon neutrophil activation [23]. Accordingly, we observed that neutrophil infection with CVB3 resulted in degradation of the NFκB inhibitor IκBα (Figure 4D), suggesting that the NFκB pathway was activated upon virus infection.

3.5 Neutrophils recognize viral infection through TLR-8

ACCEPTED MANUSCRIPT

The neutrophil effector responses triggered by CVB3 infection indicated that pathogen-recognition receptors sensed CVB3 in these cells. Because the antiviral response is mediated by endosomal TLRs [24], we first analyzed the effect of bafilomycin A1, an inhibitor of the vacuolar type H^+ATPase, and found that CVB3-induced IL-6 release was suppressed in neutrophils pretreated with bafilomycin A1 (Figure 5A). Among the different endosomal TLRs, TLR-3, TLR-7 and TLR-8, but not TLR-9 (which recognizes DNA rich in CpG motifs), might be capable of sensing CVB3 [24]. While TLR-3 is not expressed in neutrophils [25], the expression of TLR-7 and TLR-8 is still controversial [25-29]. Next, we analyzed the expression of both TLRs and the effect of neutrophil stimulation with CL264 and TL8-506, specific agonists of TLR-7 and TLR-8, respectively. While TLR-8 mRNA was highly expressed in all neutrophil samples, TLR-7 was barely expressed or not detected (Figure 5B). Accordingly, IL-6 was significantly increased upon the treatment of neutrophils with TL8-506 but not with CL264 (Figure 5C). The functionality of TLR-7 agonist was verified by stimulating peripheral blood mononuclear cells, which released IL-6 in a concentration-dependent manner upon activation with CL264 (Figure 5D). Together, these data indicate that CVB3 infection in neutrophils is mainly detected by endosomal TLR-8.

3.6 CVB3 infection increases neutrophil strategies of pathogen elimination

Pathogen elimination is a major effector response of neutrophils during infection. Therefore, we also studied whether CVB3 infection modulates three different mechanisms: granular content release, measured as MPO activity in the supernatants, the generation of ROS and NET formation. Although CVB3 infection increased MPO activity and the synthesis of ROS, the latter was not statistically significant (Figure 6A-B). We also observed that CVB3 *per se* only enhanced NETosis in a discrete manner. However, CVB3 infection markedly increased NET release in neutrophils that were previously primed by TNF-α, which by itself was not statistically significant (Figure 6 C-D). Studies by Saitoh *et*

ACCEPTED MANUSCRIPT

al. have shown that HIV induces NETosis through TLR8 activation [30]. In agreement, we found that when neutrophils were incubated with CVB3 or TNF-α (10 ng/ml) in the presence of bafilomycin A1 (50 nM), there was a significant decrease in NET formation. Moreover, stimulation of neutrophils with TL8 506, a TLR-8 agonist, triggered NETosis; this effect was significantly increased when neutrophils were previously incubated with TNF-α (Figure 6D).

3.7 Role of neutrophils in CVB3-induced myocarditis

To determine whether virus internalization by neutrophils occurs *in vivo*, mice were infected with CVB3 and, 2 days post-infection (dpi), total leukocytes were double labeled with anti-Ly6G (neutrophils) and anti-VP1 (viral antigen). Figure 7A and B showed that there were no viral infected cells in the Ly6G population. Moreover, there were no viral infected cells in the whole leukocyte population (data not shown). On the other hand, infected Vero cells were clearly positive for VP1, indicating the functionality of the assay (Figure 7B). Considering that flow cytometry was not sensitive enough to detect the presence of virus, we then performed RT-PCR and found that whole blood leukocytes contained viral RNA. Moreover, sorting of infected neutrophils demonstrated that the virus was in the $Ly6G^+$ neutrophils as well as in the $Ly6G^-$ mononuclear cells (Figure 7C).

To further clarify the role of neutrophils in acute VM, survival, viral titers and cardiac pathology were studied in infected mice without and with depletion of neutrophils by anti-Ly6G (clone 1A8) treatment. The depletion protocol achieved and maintained a depletion of blood neutrophils in a range from 96 to 99%, with minor no statistically significant effects on the percentages of lymphocytes and monocytes (Figure 8A). All mice showed a 100% survival rate. At 2 dpi, viremia was slightly reduced in the 1A8+CVB3 mice compared with the CVB3 group (Figure 8B). Similarly, cardiac viral burden at 7 dpi was also mild but significantly decreased in 1A8+CVB3 mice compared with the CVB3 group (Figure 8C).

ACCEPTED MANUSCRIPT

The histopathological analysis showed an absence of abnormalities in control mice (Figure 9A). In contrast, CVB3-infected and control isotype-infected mice showed typical multifocal myocarditis that was significantly reduced in 1A8+CVB3 mice, scoring 1.75±0.36 and 0.34±0.05, respectively (Figure 9A). Moreover, the mRNA levels of the inflammatory marker CCL-2 supported the histology data since CVB3-infected mice showed a significant increase in CCL-2 levels that were reduced in depleted animals (Figure 9B).

To characterize the inflammatory cell infiltrates, immunohistochemical studies using cell-specific antibodies for neutrophils, macrophages, and T and B lymphocytes were performed on cardiac samples from mice at 1 week p.i. (Figure 9C). Cell infiltrates, composed mainly of macrophages and T lymphocytes, were frequently associated with necrotic fibers. As expected, after depletion, neutrophils could not be detected in the infiltrates and the total number of inflammatory of cells was significantly reduced. Neutrophil depletion did not lead to major changes in the infiltrates between groups (Table I).

Using WGA staining and digital image analysis, we characterized cell size in all groups of studied animals. The results showed similar values for the control and 1A8 animal groups. Both the CVB3 and Iso+CVB3 groups showed a significant increase in cell area (Figure 9D) that was reduced in the 1A8+CVB3 group (Figure 9D), suggesting that CVB3-induced myocarditis produced reactive cardiomyocyte hypertrophy that was partially abrogated in neutrophil-depleted mice.

To determine whether CVB3 infection induced cardiomyocyte apoptosis, we performed p53 staining [31, 32]. As shown in Supplementary Figure 3, there were no significant numbers of $p53^+$ cells in the hearts of infected animals, suggesting that cardiomyocyte apoptosis was not a major event in CVB3-induced murine myocarditis. Taken together, our results indicate that neutrophil depletion leads to a decreased viral cardiac burden, neutrophil cardiac infiltration and myocarditis.

ACCEPTED MANUSCRIPT

4. Discussion

Neutrophils act as the first line of defense against harmful microorganisms. Many studies have investigated the role of neutrophils in the pathogenesis of bacterial and fungal infections [33]; however, there is much less information regarding the role of neutrophils in viral pathogenesis, particularly in viral myocarditis. In this study, we demonstrate that CVB3 is internalized by human neutrophils, and that, although the virus does not replicate, it triggers several activation effector responses and prolongs the life span of neutrophils.

After exposure to CVB3, VP1 was detected on the neutrophil surface and inside the cell. It has been reported that neutrophils do not express the CVB receptor CAR [34]; however, the fact that lymphocytes express it in very small amounts but are efficiently infected [35] and that platelets interact with CVB in a CAR-independent way [36] suggests the existence of alternative mechanisms for viral entry, at least for neutrophil cells.

Although the general concept is that neutrophils are not a target for viruses, the recent observation that influenza A targets neutrophils and is able to replicate in these cells [37] calls for a reconsideration of the role of these cells in viral infections. In this sense, neutrophils were shown to contribute to both viral clearance [30, 38] as well as viral dissemination [39, 40]. Although we found infectious viral particles in the supernatants and pellets of CVB3-infected neutrophils, the fact that these levels did not increase over time may be a result of a lack of viral replication or increased cell death due to the short half-life of neutrophils. As we found that CVB3 infection prolonged neutrophil half-life, the fact that viral RNA levels were significantly reduced after 48 hpi strongly suggests that CVB3 did not replicate in these cells.

Infection of neutrophils with CVB3 resulted in the up-regulation of CD11b, which was associated with an augmented adhesion to the extracellular matrix proteins, fibrinogen and fibronectin. Neutrophil endothelial and transepithelial migration during inflammatory

ACCEPTED MANUSCRIPT

episodes involves a complex series of adhesive interactions and signaling events. The adhesive interactions between leukocyte CD11b/CD18 and fucosylated glycoproteins expressed at basal levels, followed by binding to desmosome-associated JAM-C, are key elements of the transmigration response [41]. Thus, it might be conceivable that the up-regulation of CD11b represents a CVB3 strategy to facilitate neutrophil migration towards target organs and enhance virus dissemination.

Bacterial activated neutrophils can release granular components and chemokines, which recruit more neutrophils along with other immunocompetent cells to the site of infection [33]. Our findings showing that CVB3-infected neutrophils secreted IL-8, and that the supernatants of these infected cells promoted neutrophil migration, suggest that chemokine production by activated neutrophils is not specific to bacterial infection but instead represents a phenomenon that might also be elicited by viral infections. Of note, the chemotactic activity of supernatants from CVB3-infected cells was significantly decreased in the presence of an IL-8 blocking Ab, suggesting that IL-8 is involved in the chemotactic response of CVB3-infected neutrophils. Our findings also imply that CVB3-infected cells may be capable of directing their own recruitment to sites of inflammation and infection, thus boosting acute inflammatory responses against infection.

CVB3 infection prolonged the survival of neutrophils, associated with a marked release of IL-1β, TNF-α and IL-6, pro-inflammatory cytokines that also promote neutrophil survival [22, 42]. Interestingly, the secretion of similar cytokines upon CVB3 infection was demonstrated in early studies on human monocytes. However, in that study, the effect of cytokines on monocyte survival was not addressed [43]. The main molecular pathway involved in the release of pro-inflammatory cytokines and neutrophil survival under inflammatory conditions is NFκB [44]. Accordingly, we observed that neutrophil infection with CVB3 resulted in a marked decrease in IκBα, the inhibitory molecule of NFκB activity,

ACCEPTED MANUSCRIPT

suggesting that this signaling pathway could represent a potential target for decreasing inflammation during viral infections.

ssRNA viruses can be sensed by cytoplasmic TLR-7 and TLR-8 [45], which initiate the inflammatory response upon activation of the downstream signal NFκB. In this context, it has been reported that the CVB3-induced inflammatory response is mediated through the up-regulation and activation of cardiac TLR-8 and, to a lesser extent, TLR-7 [46]. Our data showing that inhibition of the vacuolar type ATPase impeded cytokine release, that TLR-8 but not TLR-7 is highly expressed in neutrophils and that an agonist of TLR-8 but not of TLR-**7** mimicked the IL-6 release induced by CVB3, strongly indicate that CVB3 in neutrophils is mainly recognized by TLR-8**.**

Neutrophils combat invading microorganisms by activating several strategies, including ROS generation and the release of antimicrobial molecules such as MPO and NETs [47]. Our data show that CVB3 infection triggered the secretion of MPO and NET formation. As mentioned above, viral RNA was not detected after 48 hpi. Because ROS and MPO can have direct virucidal effects, it can be speculated that these molecules could have been involved in viral degradation.

While NETs were first described as a mechanism against bacteria and fungi, several studies have recently shown that some viruses, including influenza A [48], HIV-1 [30] and hantavirus [49], trigger NET formation. Although we observed minor NET induction upon neutrophil infection with CVB3, priming the cells with the pro-inflammatory cytokine TNF-α resulted in a marked increase in extracellular DNA release. Considering that TNF-α is one of the major cytokines released from CVB3-infected monocytes [43], these findings suggest, that together with monocytes, the formation of DNA traps by neutrophils might contribute to virus elimination and/or tissue damage. In agreement with a previous study on NETs induced by HIV-1 [30], we also found that NET formation triggered by CVB3 and

ACCEPTED MANUSCRIPT

TNF-α was inhibited by bafilomycin and mimicked by a TLR8 agonist. Together, these data indicate that TLR8 is responsible for NET formation induced upon RNA virus recognition.

Although neutrophils are the first and most predominant immune cell population recruited to an affected site after tissue injury, the contribution of neutrophils to antiviral defense is much less appreciated compared to their role in bacterial or fungal infection. Neutrophils may exert beneficial as well as harmful effects during viral infections [50]. The beneficial role of neutrophils has been demonstrated in experimental models of influenza A virus (IAV) [51, 52] and herpes simplex virus 1 (HSV-1). However, it has also been shown that the excess activation of neutrophils leads to detrimental effects on the host due to the release of pro-inflammatory mediators and toxic substances that can induce pathologic features [50]. In fact, neutrophil-mediated detrimental effects, including pneumonia and respiratory distress syndrome, have been observed in IAV infections [53], stromal keratitis lesions induced by HSV [54] or liver damage in mice infected with murine Cytomegalovirus [55]. Regarding CVB3-induced VM, our results show that although all infected groups presented viral replication and myocardial necrosis, these parameters were significantly reduced in neutrophil-depleted mice. The composition of the cell infiltrate was similar to those described in other studies, with the prevalence of mononuclear cells and relatively fewer neutrophils [56-59]. Although our study has the limitation of not having used echocardiography or another functional assessment, moderate reactive hypertrophy in CVB3-infected mice was found by performing a cardiomyocyte analysis, as described by other groups [60, 61]. The detection of p53 protein expression, used to detect apoptosis [32], showed scattered p53-positive cardiomyocytes and cell exudate cells in the infected groups with no differences among them. Therefore, and in contrast to human VM [31], apoptosis does not represent a major cause of cell death in the murine model of CVB3-induced VM, in agreement with other studies [62, 63]. The reduced myocardial necrosis observed in neutrophil-depleted mice was associated with a lower viral cardiac burden.

ACCEPTED MANUSCRIPT

This reduction in cardiac viral burden was somewhat unexpected and may indicate that neutrophils directly or indirectly participate in viral dissemination. However, it should be noted that, although statistically significant, the decrease was minor, and therefore the biological significance of these data is not clear. On the other hand, the reduced inflammatory response and cardiac damage observed by histological analysis and supported by CCL-2 mRNA levels suggest that neutrophils contribute to VM development. In this sense, our *in vitro* data suggest that neutrophils can affect cardiac cells by releasing toxic pro-inflammatory mediators such as neutrophil-derived IL-1β, TNF-α, IIL-6 and IL-12 [59] that favor cell exudate accumulation**,** together with ROS and NETs, which can induce tissue damage.

In conclusion, our study demonstrates that CVB3 interacts with and activates neutrophils, endowing these innate immune cells with a relevant role in the pathogenesis of viral myocarditis. A better understanding of the role of neutrophils with respect to viral infections will reveal important information about the disease outcome and potential treatment.

Disclosures

None

Acknowledgements

We thank Vet. Hector Costa for his invaluable assistance with the animal experiments.

Funding

This work was supported by the National Agency for Scientific and Technological Promotion (CONICET, Argentina), PICT 0352/14 (MS) and PICT 1740/16 (RMG).

ACCEPTED MANUSCRIPT

ACCEPTED MANUSCRIPT

References

[1] N.J. Knowles, T. Hove, T. Hyypia, A.M.Q. King, A.M. Lindberg, M.A. Pallansch, A.C. Palmberg, P. Simmonds, T. Skern, G. Stanway, T. Yamashita, R. Zali, Virus Taxonomy:classification and Nomenclature of viruses:Ninth Report of the International Committee on Taxonomy of Viruses, in: A.M.Q. King, M.J. Adams, E.B. Carstens, E. Kefkowitz (Eds.), Elservier2012.

[2] D. Fairweather, K.A. Stafford, Y.K. Sung, Update on coxsackievirus B3 myocarditis, Curr Opin Rheumatol 24(4) (2012) 401-7.

[3] L. Andreoletti, Myocarditis, in: D. Cihakova (Ed.), InTech2011.

[4] I. Kindermann, C. Barth, F. Mahfoud, C. Ukena, M. Lenski, A. Yilmaz, K. Klingel, R. Kandolf, U. Sechtem, L.T. Cooper, M. Bohm, Update on myocarditis, J Am Coll Cardiol 59(9) (2012) 779-92.

[5] C. Gauntt, S. Huber, Coxsackievirus experimental heart diseases, Front Biosci 8 (2003) e23-35.

[6] J.F. Deniset, P. Kubes, Recent advances in understanding neutrophils, F1000Res 5 (2016) 2912.

[7] F. Wan, K. Yan, D. Xu, Q. Qian, H. Liu, M. Li, W. Xu, Vgamma1(+)gammadeltaT, early cardiac infiltrated innate population dominantly producing IL-4, protect mice against CVB3 myocarditis by modulating IFNgamma(+) T response, Mol Immunol 81 (2017) 16-25.

[8] M. Beyrau, J.V. Bodkin, S. Nourshargh, Neutrophil heterogeneity in health and disease: a revitalized avenue in inflammation and immunity, Open Biol 2(11) (2012) 120134.

[9] S. Epelman, P.P. Liu, D.L. Mann, Role of innate and adaptive immune mechanisms in cardiac injury and repair, Nat Rev Immunol 15(2) (2015) 117-29.

ACCEPTED MANUSCRIPT

[10] M.J. Lapponi, A. Carestia, V.I. Landoni, L. Rivadeneyra, J. Etulain, S. Negrotto, R.G. Pozner, M. Schattner, Regulation of neutrophil extracellular trap formation by anti-inflammatory drugs, J Pharmacol Exp Ther 345(3) (2013) 430-7.

[11] K.U. Knowlton, E.S. Jeon, N. Berkley, R. Wessely, S. Huber, A mutation in the puff region of VP2 attenuates the myocarditic phenotype of an infectious cDNA of the Woodruff variant of coxsackievirus B3, J Virol 70(11) (1996) 7811-8.

[12] J.O. Cifuente, M.F. Ferrer, C. Jaquenod de Giusti, W.C. Song, V. Romanowski, S.L. Hafenstein, R.M. Gomez, Molecular determinants of disease in coxsackievirus B1 murine infection, J Med Virol 83(9) (2011) 1571-81.

[13] C.J. De Giusti, A.E. Ure, L. Rivadeneyra, M. Schattner, R.M. Gomez, Macrophages and galectin 3 play critical roles in CVB3-induced murine acute myocarditis and chronic fibrosis, Journal of molecular and cellular cardiology 85 (2015) 58-70.

[14] S. Negrotto, H.A. Mena, A.E. Ure, C. Jaquenod De Giusti, M. Bollati-Fogolin, E.M. Vermeulen, M. Schattner, R.M. Gomez, Human Plasmacytoid Dendritic Cells Elicited Different Responses after Infection with Pathogenic and Nonpathogenic Junin Virus Strains, J Virol 89(14) (2015) 7409-13.

[15] L. Rivadeneyra, A. Carestia, J. Etulain, R.G. Pozner, C. Fondevila, S. Negrotto, M. Schattner, Regulation of platelet responses triggered by Toll-like receptor 2 and 4 ligands is another non-genomic role of nuclear factor-kappaB, Thromb Res 133(2) (2014) 235-43.

[16] R.M. Gomez, J.E. Rinehart, R. Wollmann, R.P. Roos, Theiler's murine encephalomyelitis virus-induced cardiac and skeletal muscle disease, J Virol 70(12) (1996) 8926-33.

[17] O.R. Coelho-Filho, R.V. Shah, R. Mitchell, T.G. Neilan, H. Moreno, Jr., B. Simonson, R. Kwong, A. Rosenzweig, S. Das, M. Jerosch-Herold, Quantification of cardiomyocyte hypertrophy by cardiac magnetic resonance: implications for early cardiac remodeling, Circulation 128(11) (2013) 1225-33.

ACCEPTED MANUSCRIPT

[18] D.M. Giraldo, J.C. Hernandez, P. Velilla, S. Urcuqui-Inchima, HIV-1-neutrophil interactions trigger neutrophil activation and Toll-like receptor expression, Immunol Res 64(1) (2016) 93-103.

[19] D.C. Altieri, F.R. Agbanyo, J. Plescia, M.H. Ginsberg, T.S. Edgington, E.F. Plow, A unique recognition site mediates the interaction of fibrinogen with the leukocyte integrin Mac-1 (CD11b/CD18), J Biol Chem 265(21) (1990) 12119-22.

[20] J.M. van den Berg, F.P. Mul, E. Schippers, J.J. Weening, D. Roos, T.W. Kuijpers, Beta1 integrin activation on human neutrophils promotes beta2 integrin-mediated adhesion to fibronectin, Eur J Immunol 31(1) (2001) 276-84.

[21] M. Bickel, The role of interleukin-8 in inflammation and mechanisms of regulation, J Periodontol 64(5 Suppl) (1993) 456-60.

[22] F. Colotta, F. Re, N. Polentarutti, S. Sozzani, A. Mantovani, Modulation of granulocyte survival and programmed cell death by cytokines and bacterial products, Blood 80(8) (1992) 2012-20.

[23] P.P. McDonald, Transcriptional regulation in neutrophils: teaching old cells new tricks, Adv Immunol 82 (2004) 1-48.

[24] L.A. O'Neill, D. Golenbock, A.G. Bowie, The history of Toll-like receptors - redefining innate immunity, Nat Rev Immunol 13(6) (2013) 453-60.

[25] F. Hayashi, T.K. Means, A.D. Luster, Toll-like receptors stimulate human neutrophil function, Blood 102(7) (2003) 2660-9.

[26] M. Janke, J. Poth, V. Wimmenauer, T. Giese, C. Coch, W. Barchet, M. Schlee, G. Hartmann, Selective and direct activation of human neutrophils but not eosinophils by Toll-like receptor 8, J Allergy Clin Immunol 123(5) (2009) 1026-33.

[27] M. Zimmermann, F. Arruda-Silva, F. Bianchetto-Aguilera, G. Finotti, F. Calzetti, P. Scapini, C. Lunardi, M.A. Cassatella, N. Tamassia, IFNalpha enhances the production of IL-6 by human neutrophils activated via TLR8, Sci Rep 6 (2016) 19674.

ACCEPTED MANUSCRIPT

[28] H. Nagase, S. Okugawa, Y. Ota, M. Yamaguchi, H. Tomizawa, K. Matsushima, K. Ohta, K. Yamamoto, K. Hirai, Expression and function of Toll-like receptors in eosinophils: activation by Toll-like receptor 7 ligand, J Immunol 171(8) (2003) 3977-82.

[29] J.P. Wang, G.N. Bowen, C. Padden, A. Cerny, R.W. Finberg, P.E. Newburger, E.A. Kurt-Jones, Toll-like receptor-mediated activation of neutrophils by influenza A virus, Blood 112(5) (2008) 2028-34.

[30] T. Saitoh, J. Komano, Y. Saitoh, T. Misawa, M. Takahama, T. Kozaki, T. Uehata, H. Iwasaki, H. Omori, S. Yamaoka, N. Yamamoto, S. Akira, Neutrophil extracellular traps mediate a host defense response to human immunodeficiency virus-1, Cell Host Microbe 12(1) (2012) 109-16.

[31] A. Tsipis, A.M. Athanassiadou, P. Athanassiadou, N. Kavantzas, G. Agrogiannis, E. Patsouris, Apoptosis-related factors p53, bcl-2 and the defects of force transmission in dilated cardiomyopathy, Pathol Res Pract 206(9) (2010) 625-30.

[32] Y. Shen, E. White, p53-dependent apoptosis pathways, Adv Cancer Res 82 (2001) 55-84.

[33] C. Tecchio, M.A. Cassatella, Neutrophil-derived chemokines on the road to immunity, Semin Immunol 28(2) (2016) 119-28.

[34] M.J. Cotter, A.K. Zaiss, D.A. Muruve, Neutrophils interact with adenovirus vectors via Fc receptors and complement receptor 1, J Virol 79(23) (2005) 14622-31.

[35] I. Mena, C.M. Perry, S. Harkins, F. Rodriguez, J. Gebhard, J.L. Whitton, The role of B lymphocytes in coxsackievirus B3 infection, Am J Pathol 155(4) (1999) 1205-15.

[36] S. Negrotto, C. Jaquenod de Giusti, L. Rivadeneyra, A.E. Ure, H.A. Mena, M. Schattner, R.M. Gomez, Platelets interact with Coxsackieviruses B and have a critical role in the pathogenesis of virus-induced myocarditis, J Thromb Haemost 13(2) (2015) 271-82.

ACCEPTED MANUSCRIPT

[37] Z. Zhang, T. Huang, F. Yu, X. Liu, C. Zhao, X. Chen, D.J. Kelvin, J. Gu, Infectious Progeny of 2009 A (H1N1) Influenza Virus Replicated in and Released from Human Neutrophils, Sci Rep 5 (2015) 17809.

[38] C.N. Jenne, C.H. Wong, F.J. Zemp, B. McDonald, M.M. Rahman, P.A. Forsyth, G. McFadden, P. Kubes, Neutrophils recruited to sites of infection protect from virus challenge by releasing neutrophil extracellular traps, Cell Host Microbe 13(2) (2013) 169-80.

[39] J.E. Grundy, K.M. Lawson, L.P. MacCormac, J.M. Fletcher, K.L. Yong, Cytomegalovirus-infected endothelial cells recruit neutrophils by the secretion of C-X-C chemokines and transmit virus by direct neutrophil-endothelial cell contact and during neutrophil transendothelial migration, J Infect Dis 177(6) (1998) 1465-74.

[40] D. Ratcliffe, G. Migliorisi, E. Cramer, Translocation of influenza virus by migrating neutrophils, Cell Mol Biol 38(1) (1992) 63-70.

[41] Y. Liu, S.K. Shaw, S. Ma, L. Yang, F.W. Luscinskas, C.A. Parkos, Regulation of leukocyte transmigration: cell surface interactions and signaling events, J Immunol 172(1) (2004) 7-13.

[42] J. Maggini, S. Raiden, G. Salamone, A. Trevani, J. Geffner, Regulation of neutrophil apoptosis by cytokines, pathogens and environmental stressors, Front Biosci (Landmark Ed) 14 (2009) 2372-85.

[43] A. Henke, C. Mohr, H. Sprenger, C. Graebner, A. Stelzner, M. Nain, D. Gemsa, Coxsackievirus B3-induced production of tumor necrosis factor-alpha, IL-1 beta, and IL-6 in human monocytes, J Immunol 148(7) (1992) 2270-7.

[44] S.R. Walmsley, C. Print, N. Farahi, C. Peyssonnaux, R.S. Johnson, T. Cramer, A. Sobolewski, A.M. Condliffe, A.S. Cowburn, N. Johnson, E.R. Chilvers, Hypoxia-induced neutrophil survival is mediated by HIF-1alpha-dependent NF-kappaB activity, J Exp Med 201(1) (2005) 105-15.

ACCEPTED MANUSCRIPT

[45] F. Heil, H. Hemmi, H. Hochrein, F. Ampenberger, C. Kirschning, S. Akira, G. Lipford, H. Wagner, S. Bauer, Species-specific recognition of single-stranded RNA via toll-like receptor 7 and 8, Science 303(5663) (2004) 1526-9.

[46] K. Triantafilou, G. Orthopoulos, E. Vakakis, M.A. Ahmed, D.T. Golenbock, P.M. Lepper, M. Triantafilou, Human cardiac inflammatory responses triggered by Coxsackie B viruses are mainly Toll-like receptor (TLR) 8-dependent, Cell Microbiol 7(8) (2005) 1117-26.

[47] E. Kolaczkowska, P. Kubes, Neutrophil recruitment and function in health and inflammation, Nat Rev Immunol 13(3) (2013) 159-75.

[48] T. Narasaraju, E. Yang, R.P. Samy, H.H. Ng, W.P. Poh, A.A. Liew, M.C. Phoon, N. van Rooijen, V.T. Chow, Excessive neutrophils and neutrophil extracellular traps contribute to acute lung injury of influenza pneumonitis, Am J Pathol 179(1) (2011) 199-210.

[49] M.J. Raftery, P. Lalwani, E. Krautkrmer, T. Peters, K. Scharffetter-Kochanek, R. Kruger, J. Hofmann, K. Seeger, D.H. Kruger, G. Schonrich, beta2 integrin mediates hantavirus-induced release of neutrophil extracellular traps, J Exp Med 211(7) (2014) 1485-97.

[50] I.E. Galani, E. Andreakos, Neutrophils in viral infections: Current concepts and caveats, J Leukoc Biol 98(4) (2015) 557-64.

[51] M.D. Tate, Y.M. Deng, J.E. Jones, G.P. Anderson, A.G. Brooks, P.C. Reading, Neutrophils ameliorate lung injury and the development of severe disease during influenza infection, J Immunol 183(11) (2009) 7441-50.

[52] T.M. Tumpey, A. Garcia-Sastre, J.K. Taubenberger, P. Palese, D.E. Swayne, M.J. Pantin-Jackwood, S. Schultz-Cherry, A. Solorzano, N. Van Rooijen, J.M. Katz, C.F. Basler, Pathogenicity of influenza viruses with genes from the 1918 pandemic virus: functional

ACCEPTED MANUSCRIPT

roles of alveolar macrophages and neutrophils in limiting virus replication and mortality in mice, J Virol 79(23) (2005) 14933-44.

[53] J.V. Camp, C.B. Jonsson, A Role for Neutrophils in Viral Respiratory Disease, Front Immunol 8 (2017) 550.

[54] N.K. Rajasagi, P.B. Reddy, A. Suryawanshi, S. Mulik, P. Gjorstrup, B.T. Rouse, Controlling herpes simplex virus-induced ocular inflammatory lesions with the lipid-derived mediator resolvin E1, J Immunol 186(3) (2011) 1735-46.

[55] H.W. Stout-Delgado, W. Du, A.C. Shirali, C.J. Booth, D.R. Goldstein, Aging promotes neutrophil-induced mortality by augmenting IL-17 production during viral infection, Cell Host Microbe 6(5) (2009) 446-56.

[56] A. Henke, S. Huber, A. Stelzner, J.L. Whitton, The role of CD8+ T lymphocytes in coxsackievirus B3-induced myocarditis, J Virol 69(11) (1995) 6720-8.

[57] D. Cihakova, N.R. Rose, Pathogenesis of myocarditis and dilated cardiomyopathy, Adv Immunol 99 (2008) 95-114.

[58] Y. Seko, Findings in Murine Viral Myocarditis, in: J. Milei (Ed.), Diagnosis and Treatment of Myocarditis, InTech2013, pp. 65-80.

[59] D. Fairweather, S. Frisancho-Kiss, S.A. Yusung, M.A. Barrett, S.E. Davis, R.A. Steele, S.J. Gatewood, N.R. Rose, IL-12 protects against coxsackievirus B3-induced myocarditis by increasing IFN-gamma and macrophage and neutrophil populations in the heart, J Immunol 174(1) (2005) 261-9.

[60] J. Sin, J.M. Puccini, C. Huang, M.H. Konstandin, P.E. Gilbert, M.A. Sussman, R.A. Gottlieb, R. Feuer, The impact of juvenile coxsackievirus infection on cardiac progenitor cells and postnatal heart development, PLoS Pathog 10(7) (2014) e1004249.

[61] J.A. Onyimba, M.J. Coronado, A.E. Garton, J.B. Kim, A. Bucek, D. Bedja, K.L. Gabrielson, T.R. Guilarte, D. Fairweather, The innate immune response to coxsackievirus

ACCEPTED MANUSCRIPT

B3 predicts progression to cardiovascular disease and heart failure in male mice, Biol Sex Differ 2 (2011) 2.

[62] J.T. Colston, B. Chandrasekar, G.L. Freeman, Expression of apoptosis-related proteins in experimental coxsackievirus myocarditis, Cardiovasc Res 38(1) (1998) 158-68.

[63] A. Henke, H. Launhardt, K. Klement, A. Stelzner, R. Zell, T. Munder, Apoptosis in coxsackievirus B3-caused diseases: interaction between the capsid protein VP2 and the proapoptotic protein siva, J Virol 74(9) (2000) 4284-90.

ACCEPTED MANUSCRIPT

ACCEPTED MANUSCRIPT

Figure 1. Coxsackievirus B3 (CVB3) interacts with neutrophils. Human neutrophils and Vero cells were uninfected or infected with CVB3, and the presence of viral particles was detected at 1 or 24 h hpi. Monolayer of infected Vero cells shows 100% cytopathology by 24 hpi. A) The expression of the enterovirus protein VP1 was determined by immunofluorescence and analyzed by confocal microscopy. Original magnification 60x (scale bar: 20 μm). B) Surface (non-permeabilized cells) and intracellular VP1 expression (permeabilized cells) were determined by flow cytometry. The images are representative of three independent experiments.

Figure 2. CVB3 does not replicate in neutrophils. A) Vero cells and neutrophils were infected with CVB3 (MOI 1), and plaque-forming units (PFU) in the supernatants (Sup) and pellets were quantified at different times pi by the infectivity titration assay in Vero cells. B) CVB3 mRNA (RNA) was detected by RT-PCR. The results are the mean±SEM of three independent experiments (*****P*<0.0001 vs 1 hpi).

Figure 3. CVB3 interaction with neutrophils triggers adhesion and migration responses. All responses were determined in non-infected (control and mock) and infected neutrophils A) CD11b expression was determined by flow cytometry, and the results were expressed as the mean fluorescence intensity (MFI). B) Neutrophils were seeded on fibrinogen or fibronectin coated-wells, and 3 h later, adhesion was evaluated by phosphatase acid activity quantification. AU: arbitrary units. C) IL-8 levels were determined in the supernatants after 18 h of infection. D) Neutrophil chemotaxis was quantified using the Boyden chamber technique. The cells were placed in the upper wells, and the supernatant from infected (incubated with IgG or anti-IL-8) or non-infected neutrophils was added to the lower wells. The number of neutrophils that migrated through the filter was counted in the five random higher-power fields (400x). The results are the mean±SEM of four to five independent experiments (**P* < 0.05, ***P* < 0.01, ****P* < 0.001 and *****P* < 0.0001 vs control; ##*P* < 0.01 and ###P<0.001).

ACCEPTED MANUSCRIPT

Figure 4. Neutrophil infection with CVB3 inhibits apoptosis, induces cytokine release and activates transcription factor NFκB. All responses were determined in non-infected (control and mock) and infected neutrophils. The percentage of apoptotic cells was evaluated by A) monitoring nuclear morphology changes and viability by labelling cells with a mixture of acridine orange and ethidium bromide (100 µg/ml) and B) detection of hypodiploid cells by flow cytometry. C) The release of IL-1β, TNF-α and IL-6 was determined in the supernatants 18 h after virus infection by ELISA. IL-6 levels were also analyzed in cells infected with UV-inactivated virus (i-CVB3). D) Activation of NFκB was evaluated by degradation of its inhibitor IκBα by Western blotting. The results are the mean±SEM of three to five independent experiments (**P* < 0.05 and ***P* < 0.01 vs. control, #*P* < 0.05 and ##*P* < 0.01).

Figure 5. Neutrophils sense viral infection through TLR-8. A) IL-6 secretion was measured by ELISA in the supernatants of neutrophils infected with CVB3 in the absence or presence of bafilomycin A1 (50 nM). B), an inhibitor of vacuolar type H^+ATPase. Neutrophil mRNAs encoding TLR-7 and TLR-8 were detected by RT-PCR in cells from three independent donors. Peripheral blood mononuclear cells (PBMC) were used as the positive control for TLR-7 and TLR-8. C) IL-6 release was measured in the supernatants of neutrophils that were stimulated for 18 h with different concentrations of TL8-506 and CL264, which are TLR-8 and TLR-7 agonists, respectively. D) IL-6 levels detected in the supernatants of peripheral blood mononuclear cells that were stimulated with different concentrations of CL264. The results are the mean±SEM of three to six independent experiments (***P* 0.01 < vs. Mock, **P* < 0.05, and ****P* 0.001 < vs. None and ##*P* < 0.01).

Figure 6. Neutrophil effector responses induced by CVB3 infection. Effector responses were determined in non-infected (control and mock) and infected neutrophils. A) Myeloperoxidase (MPO) activity was measured in supernatants after 3 h of infection. B) Reactive oxygen species (ROS) generation was evaluated by flow cytometry by labelling

ACCEPTED MANUSCRIPT

cells with dihydrorhodamine. C) NET formation was evaluated by incubating neutrophils for 3 h with CVB3 at MOI of 1 and with or without TNF-α (10 ng/ml). The cells were then fixed, permeabilized, stained with PI for DNA (red) and the specific marker anti-human neutrophil elastase (HNE, green) and visualized by confocal fluorescence microscopy. Original magnification, 60x (scale bar: 20 µm). D) Neutrophils were incubated with CVB3, TNF-α or TNF-α (10 ng/ml) plus CVB3 (MOI=1) in the absence or presence of bafilomycin A1 (50 nM), after which the DNA was quantified in the supernatants by fluorometry. TL8 506 was used as a TLR-8 agonist. The results are the mean±SEM of four to five independent experiments (*P < 0.05, and ***P < 0.001 vs. control, #P < 0.05 and ##P < 0.01**).**

Figure 7. CVB3 internalization by neutrophils in infected mouse A) Representative flow cytometry dot plots of $Ly6G^+$ neutrophils (G1) in peripheral white blood cells (WBC) from non-infected and infected mice at 2 dpi. B) Representative histogram graphs of VP1 of G1 from non-infected and infected mice and Vero cells (positive control of VP1 staining). C) CVB3 mRNA (RNA) was detected by RT-PCR in WBC from non-infected (1) and: total (2), sorted $Ly6G^+$neutrophils (3) or sorted $Ly6G^-$ mononuclear cells (4) from WBC infected mice. A representative of three independent experiments is shown.

Figure 8. Neutrophil depletion mildly decreases viremia and heart viral titers. Neutrophil depletion was induced by intra-peritoneal inoculation with 100 µl of PBS containing 100 µg of anti-Ly6G (1A8) every 24 h. Control mice were inoculated with an isotype Ab (clone 2A3) under the same conditions. The first inoculation was performed one day before infection and then every 24 h. The mice were infected intraperitoneally with $2x10^5$ PFU of virus in 200 µl of PBS (CVB3) and 100 µg of isotype (Iso+CVB3) or 1A8 (1A8+CVB3). A) Hematological counts were performed using a veterinary hematological analyzer. B) Blood was collected by retro-orbital venous puncture and viremia was determined in plasma samples at 2 dpi. C) At day 7 pi, the infectivity titers were determined in heart tissue by a plaque-forming unit (PFU) assay. The results are the

ACCEPTED MANUSCRIPT

mean±SEM of five independent experiments (*** $P < 0.001$ vs. control, ## $P < 0.01$). ND=not detected.

Figure 9. Neutrophil depletion decreases the severity of CVB3-induced myocarditis by reducing cardiomyocyte area, gene expression of CCL-2 and total inflammatory cell infiltration in the heart. A) Representative images of hematoxylin/eosin-stained sections from murine hearts collected at 7 dpi (original magnification 100x and 400x and squares indicate myocarditic lesions) and assessed by blinded histopathological scoring of myocarditis lesions was performed by optical microscopic examination of cardiac sections. B) mRNA expression levels of CCL-2 were measured by qPCR at 7 dpi in murine hearts. C) Representative images of immunohistochemical studies using cell-specific antibodies from cardiac muscle samples at 7 dpi. 1A8 (neutrophils); Mac-2 (macrophages); CD45R (B lymphocytes); CD4 and CD8 (T lymphocytes). Scale bar represents 25 µm. D) Representative pictures of WGA-stained myocardial cross sections and quantitative analysis of cardiomyocyte cross-sectional area. Scale bar represents 25 µm. The results are the mean±SEM of five independent experiments. (**P < 0.01 and ****P < 0.0001 vs control; ##P < 0.01 and ####P<0.0001). ND=not detected.

ACCEPTED MANUSCRIPT

ACCEPTED MANUSCRIPT

Table I. Cardiac cell infiltrate composition.

Total cells	**Neutrophils** (% of total cells)	**Macrophages** (% of total cells)	**T Lymphocytes** (% of total cells)	**B Lymphocytes** (% of total cells)
CVB3 (182±25 cells)	11±2	42±4	37±2 (16% CD4, 21% CD8)	10±1
CVB3+Iso (175±20 cells)	10±2	40±4	39±2 (16% CD4, 21% CD8)	11±1
CVB3+1A8 (95±15* cells)	0	44±3	44±4 (20% CD4, 25% CD8)	12±2%

*P<0.05, n=3

ACCEPTED MANUSCRIPT

ACCEPTED MANUSCRIPT

Highlights

-Coxsackievirus B3 (CVB3) interacts with, but does not replicate in human neutrophils.

-CVB3 increases neutrophil survival, CD11b expression, cytokine and IL-8 release.

-CVB3 triggers neutrophil release of myeloperoxidase and NETs.

-Neutrophils sense CVB3 mainly through TLR-8 and the activation of NFκB.

-Neutrophil-depleted CVB3-infected mice exhibit reduced viral myocarditis.

ACCEPTED MANUSCRIPT

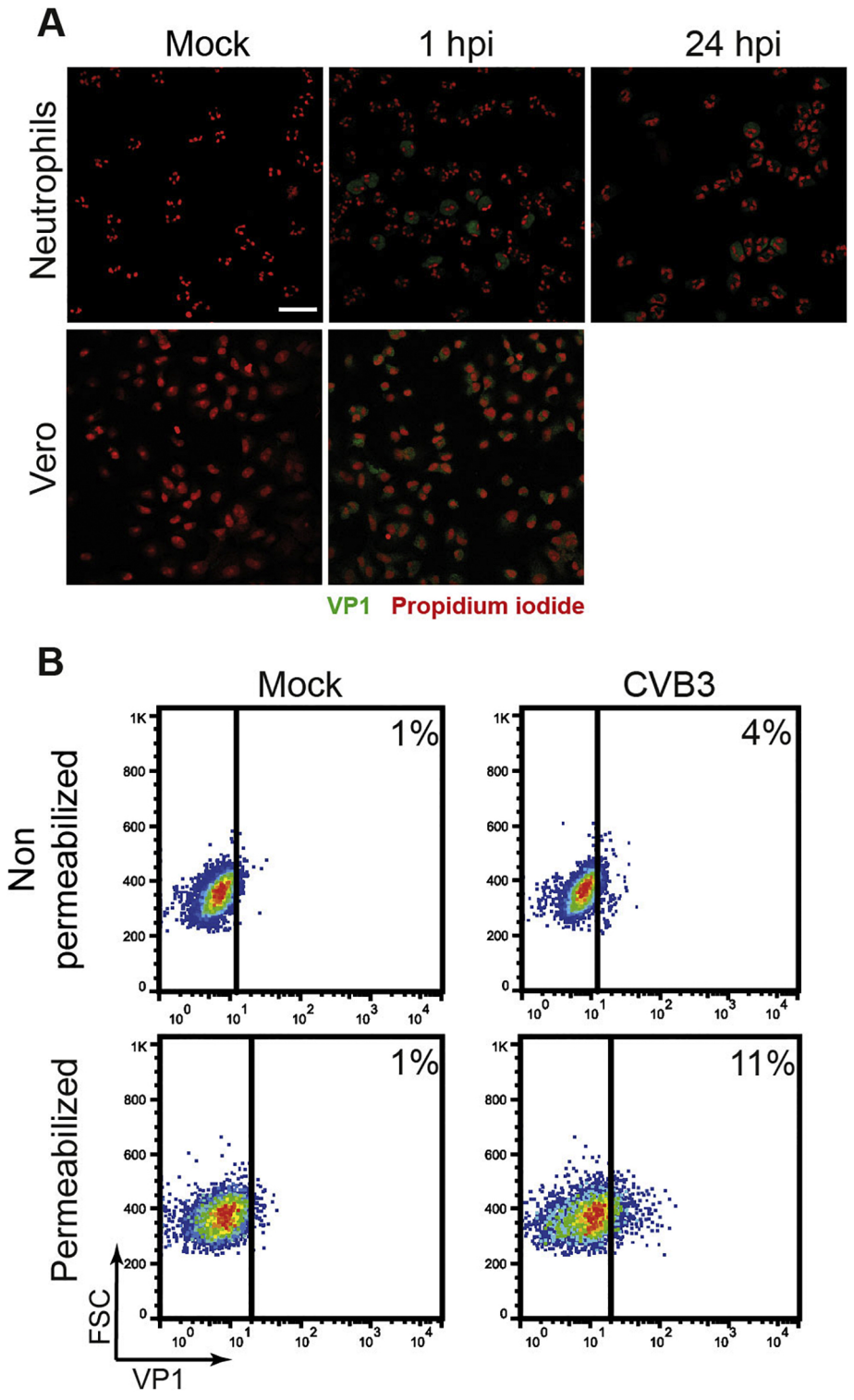
A
Mock
1 hpi
24 hpi
Neutrophils
Vero
VP1 Propidium iodide
B
Mock
CVB3
Non permeabilized
Permeabilized
1%
4%
1%
11%
FSC
VP1

Figure 1

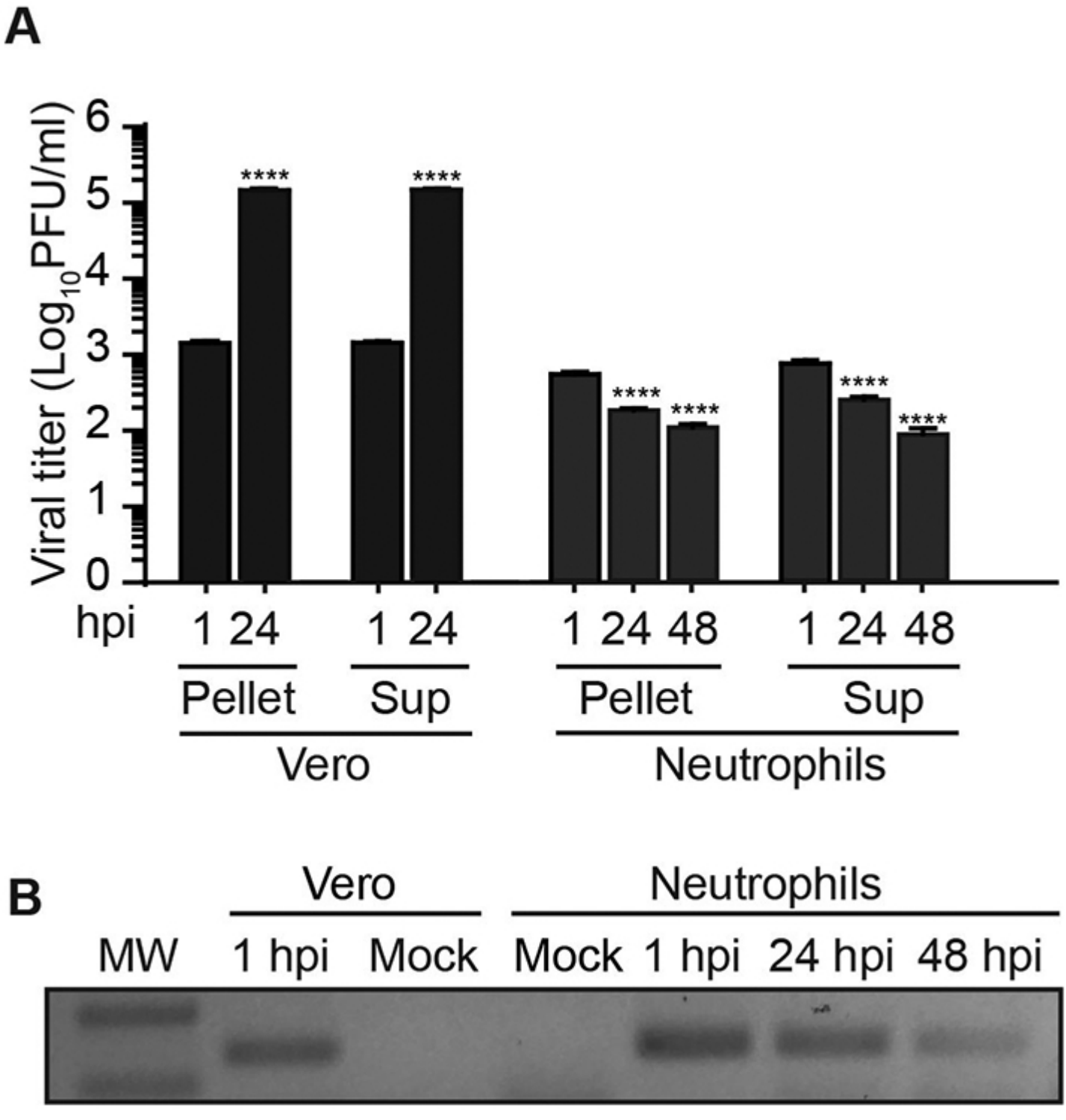
A
Viral titer (Log10PFU/ml)
0
1
2
3
4
5
6
****
****
****
****
****
****
hpi
1 24
1 24
1 24 48
1 24 48
Pellet
Sup
Pellet
Sup
Vero
Neutrophils
B
Vero
Neutrophils
MW
1 hpi
Mock
Mock
1 hpi
24 hpi
48 hpi

Figure 2

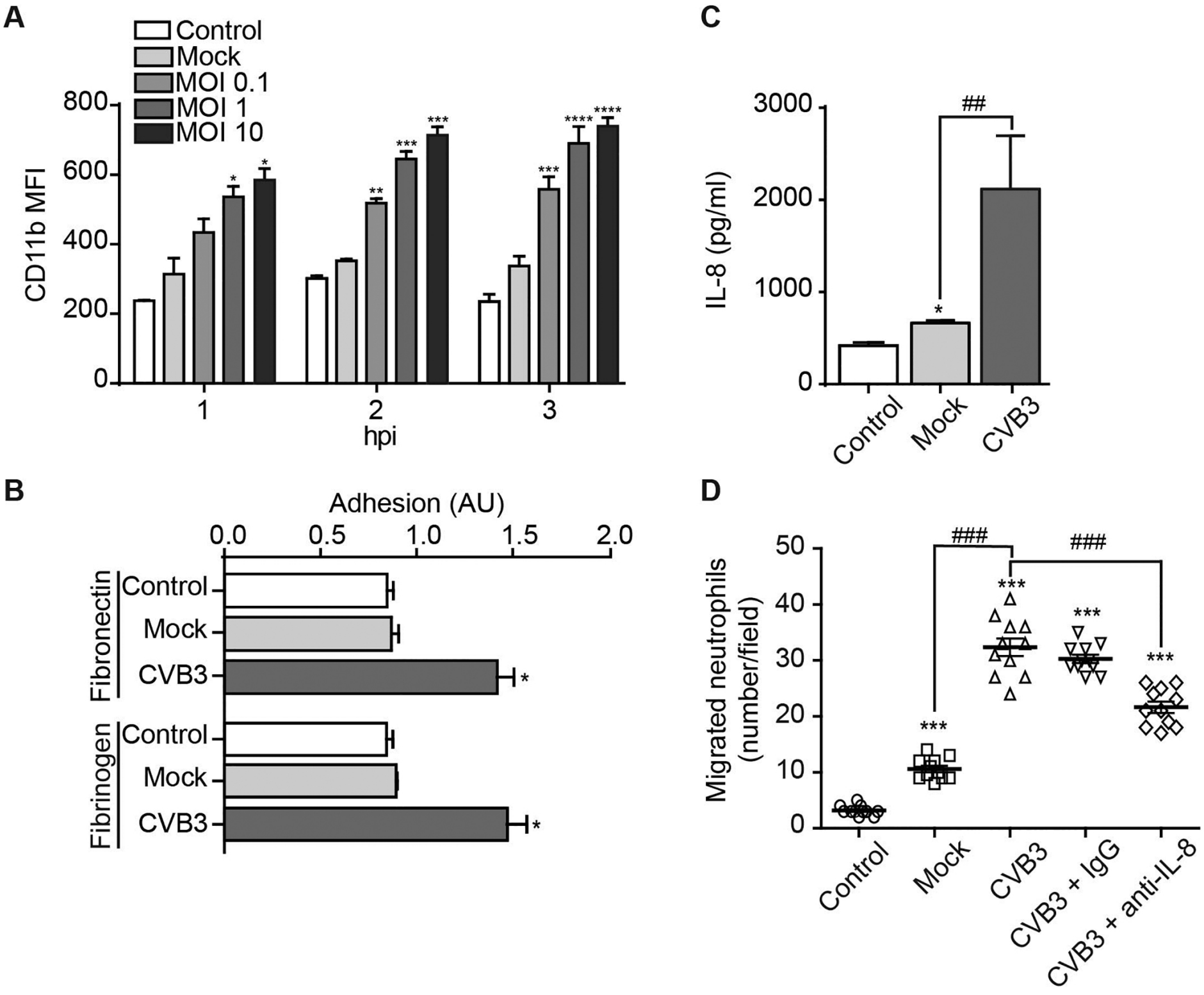
A
Control
Mock
MOI 0.1
MOI 1
MOI 10
CD11b MFI
800
600
400
200
0
1
2
3
hpi
B
Adhesion (AU)
0.0
0.5
1.0
1.5
2.0
Fibronectin
Control
Mock
CVB3
Fibrinogen
Control
Mock
CVB3
C
IL-8 (pg/ml)
3000
2000
1000
0
Control
Mock
CVB3
D
Migrated neutrophils (number/field)
50
40
30
20
10
0
Control
Mock
CVB3
CVB3 + IgG
CVB3 + anti-IL-8

Figure 3

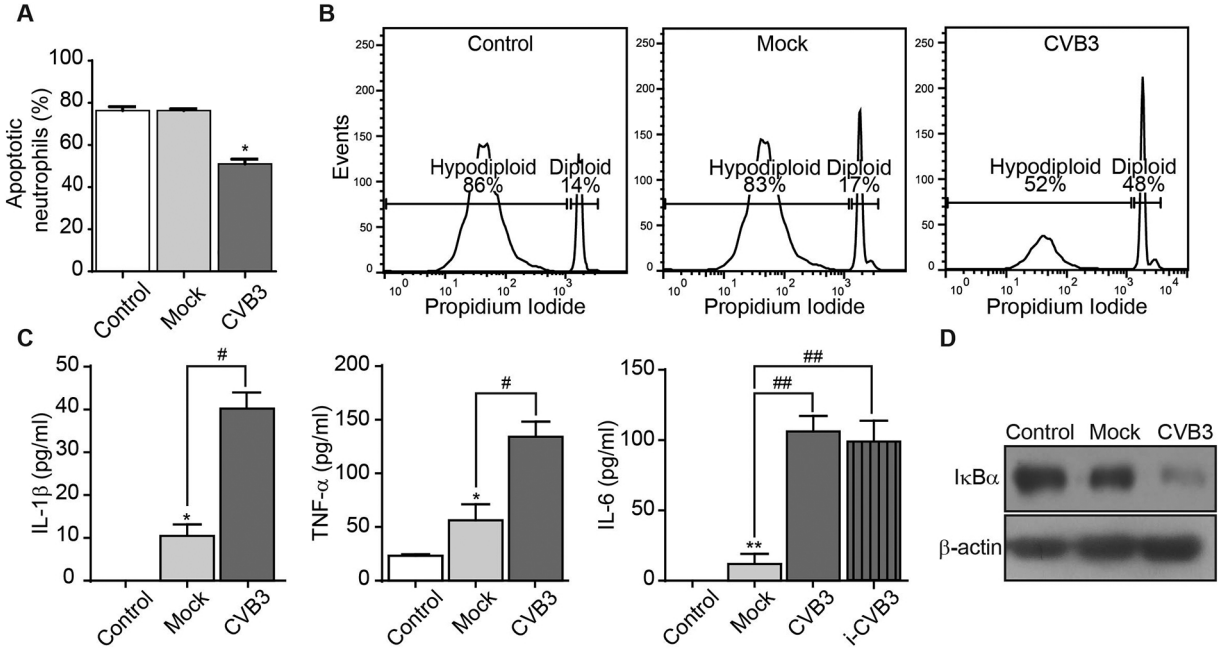
A
Apoptotic neutrophils (%)
100
80
60
40
20
0
*
Control
Mock
CVB3
B
Control
Mock
CVB3
Events
Hypodiploid 86%
Diploid 14%
Hypodiploid 83%
Diploid 17%
Hypodiploid 52%
Diploid 48%
Propidium Iodide
C
IL-1β (pg/ml)
TNF-α (pg/ml)
IL-6 (pg/ml)
#
##
*
**
Control
Mock
CVB3
i-CVB3
D
Control
Mock
CVB3
IκBα
β-actin

Figure 4

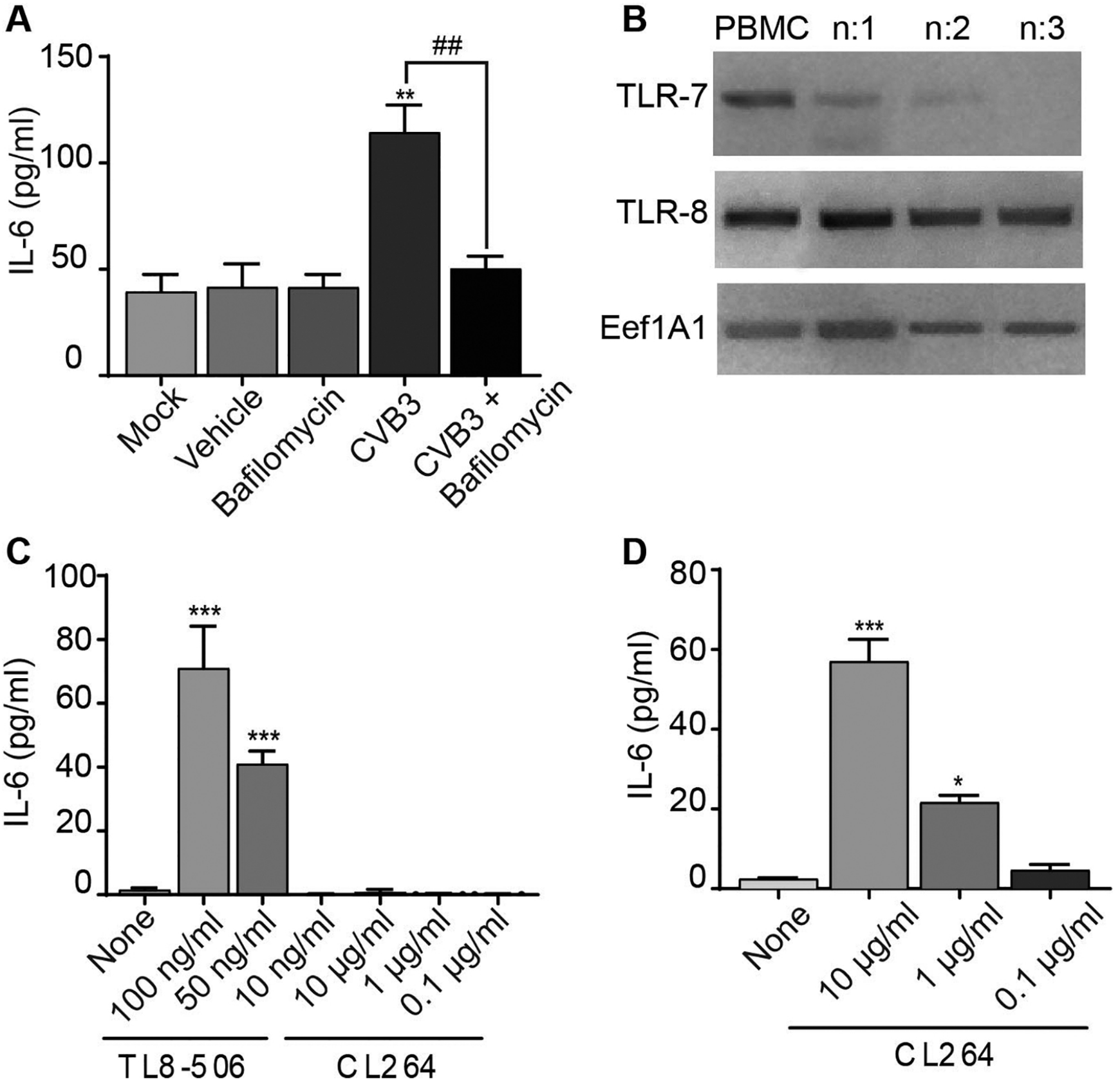
A
IL-6 (pg/ml)
150
100
50
0
**
##
Mock
Vehicle
Bafilomycin
CVB3
CVB3 + Bafilomycin
B
PBMC
n:1
n:2
n:3
TLR-7
TLR-8
Eef1A1
C
IL-6 (pg/ml)
100
80
60
40
20
0
***
***
None
100 ng/ml
50 ng/ml
10 ng/ml
10 µg/ml
1 µg/ml
0.1 µg/ml
TL8-506
CL264
D
IL-6 (pg/ml)
80
60
40
20
0
***
*
None
10 µg/ml
1 µg/ml
0.1 µg/ml
CL264

Figure 5

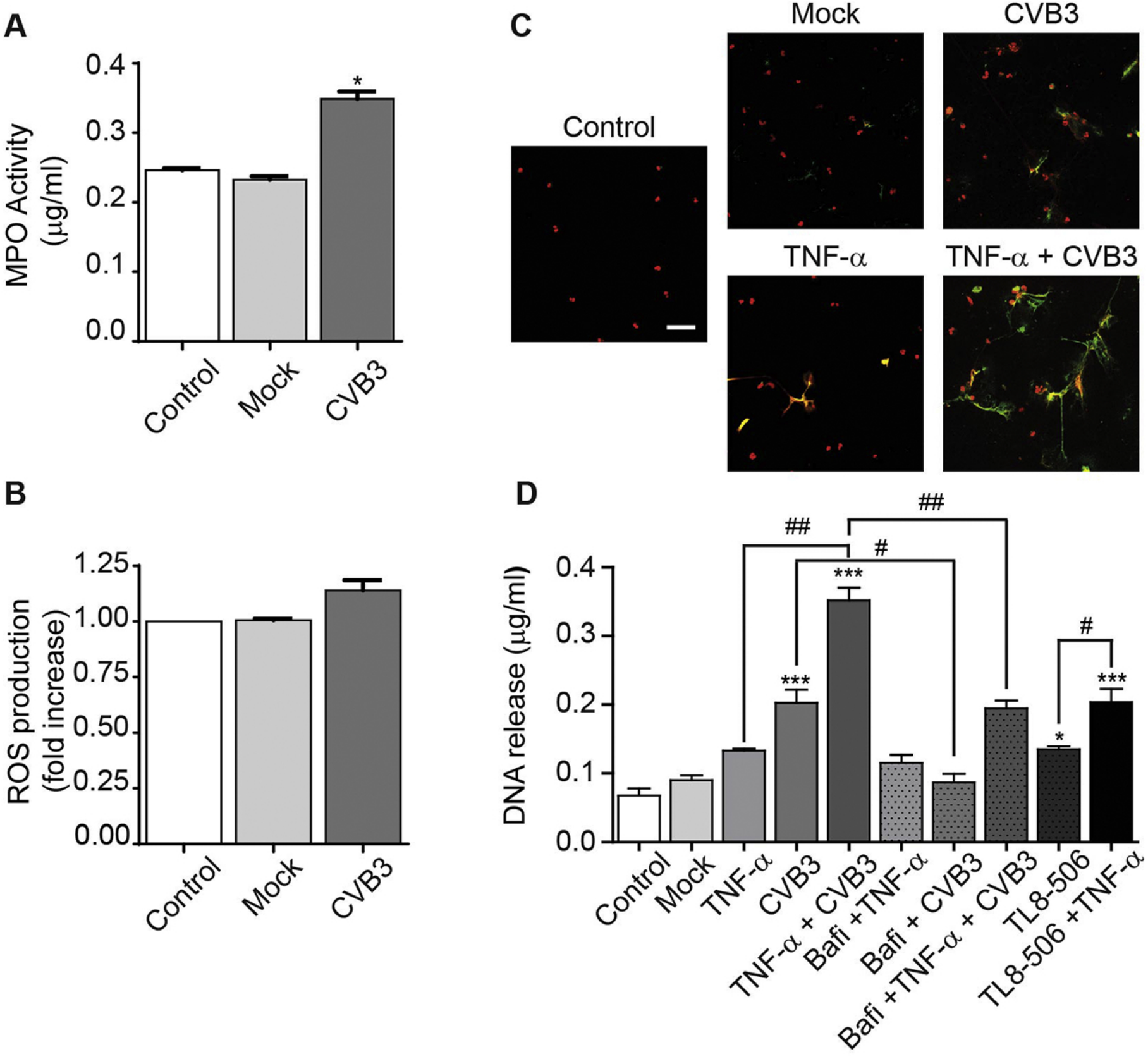
A
MPO Activity (μg/ml)
0.4
0.3
0.2
0.1
0.0
*
Control
Mock
CVB3
B
ROS production (fold increase)
1.25
1.00
0.75
0.50
0.25
0.00
Control
Mock
CVB3
C
Control
Mock
CVB3
TNF-α
TNF-α + CVB3
D
DNA release (μg/ml)
0.4
0.3
0.2
0.1
0.0
##
#
***
***
*
Control
Mock
TNF-α
CVB3
TNF-α + CVB3
Bafi +TNF-α
Bafi + CVB3
Bafi +TNF-α + CVB3
TL8-506
TL8-506 +TNF-α

Figure 6

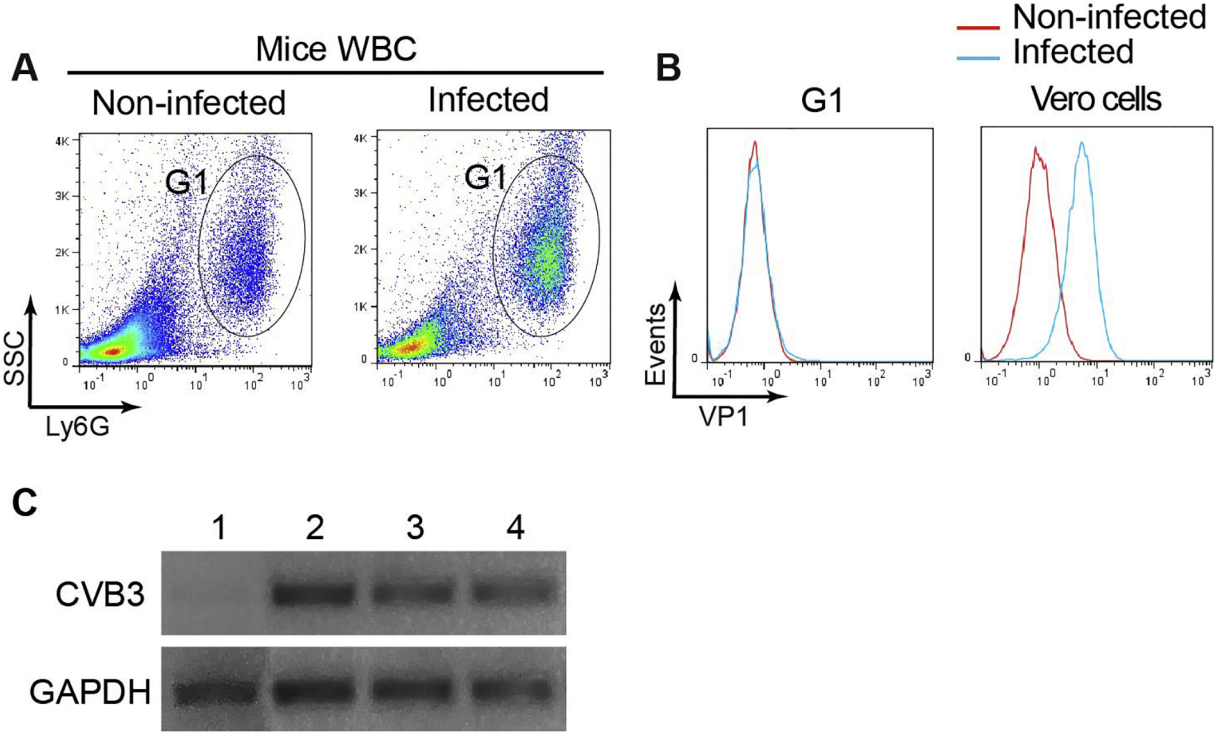
A
Mice WBC
Non-infected
Infected
G1
G1
SSC
Ly6G
B
Non-infected
Infected
G1
Vero cells
Events
VP1
C
1
2
3
4
CVB3
GAPDH

Figure 7

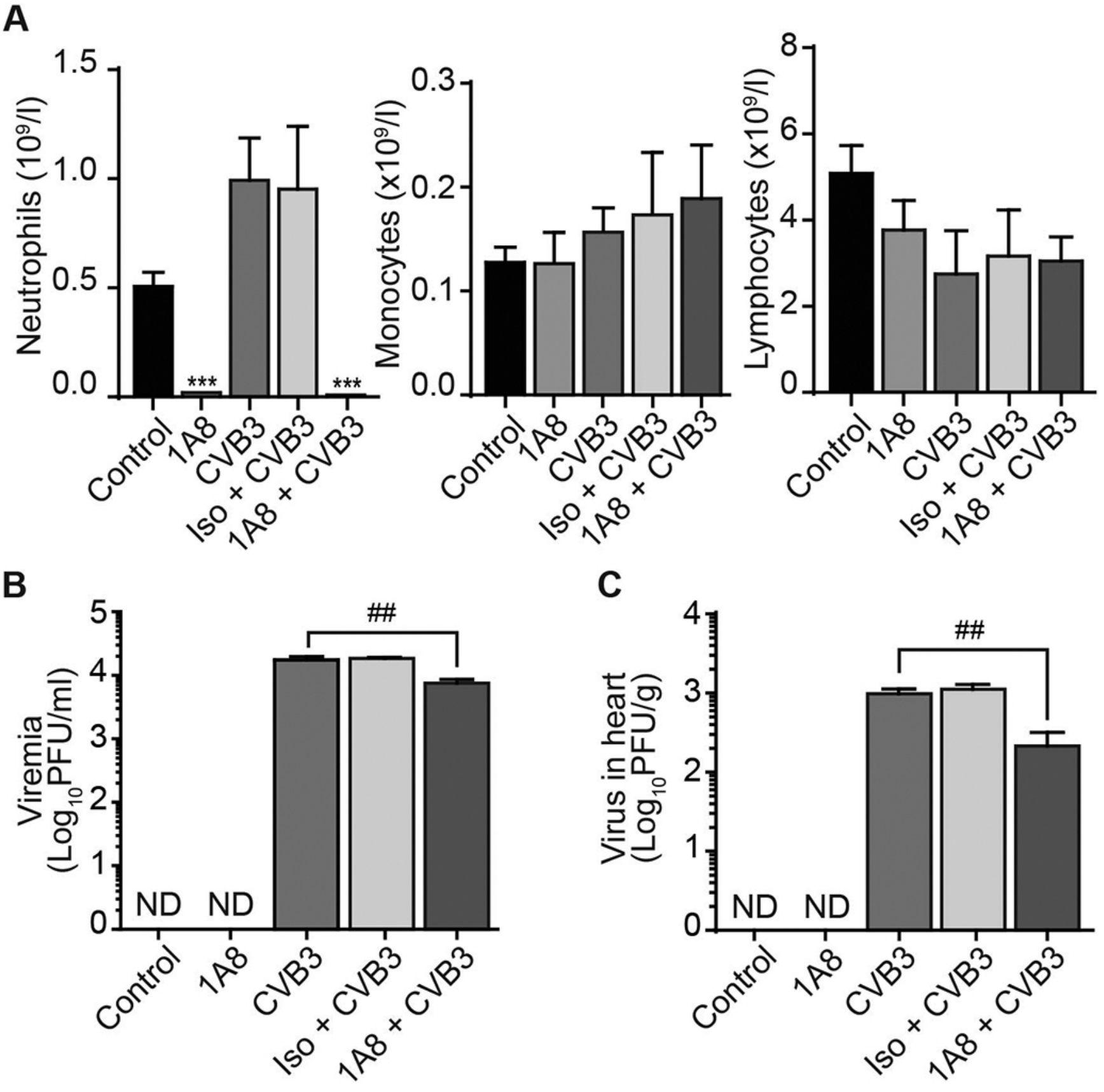
A
Neutrophils (10⁹/l)
1.5
1.0
0.5
0.0
***
***
Monocytes (x10⁹/l)
0.3
0.2
0.1
0.0
Lymphocytes (x10⁹/l)
8
6
4
2
0
Control
1A8
CVB3
Iso + CVB3
1A8 + CVB3
B
Viremia (Log10PFU/ml)
5
4
3
2
1
0
##
ND
ND
C
Virus in heart (Log10PFU/g)
4
3
2
1
0
##
ND
ND

Figure 8

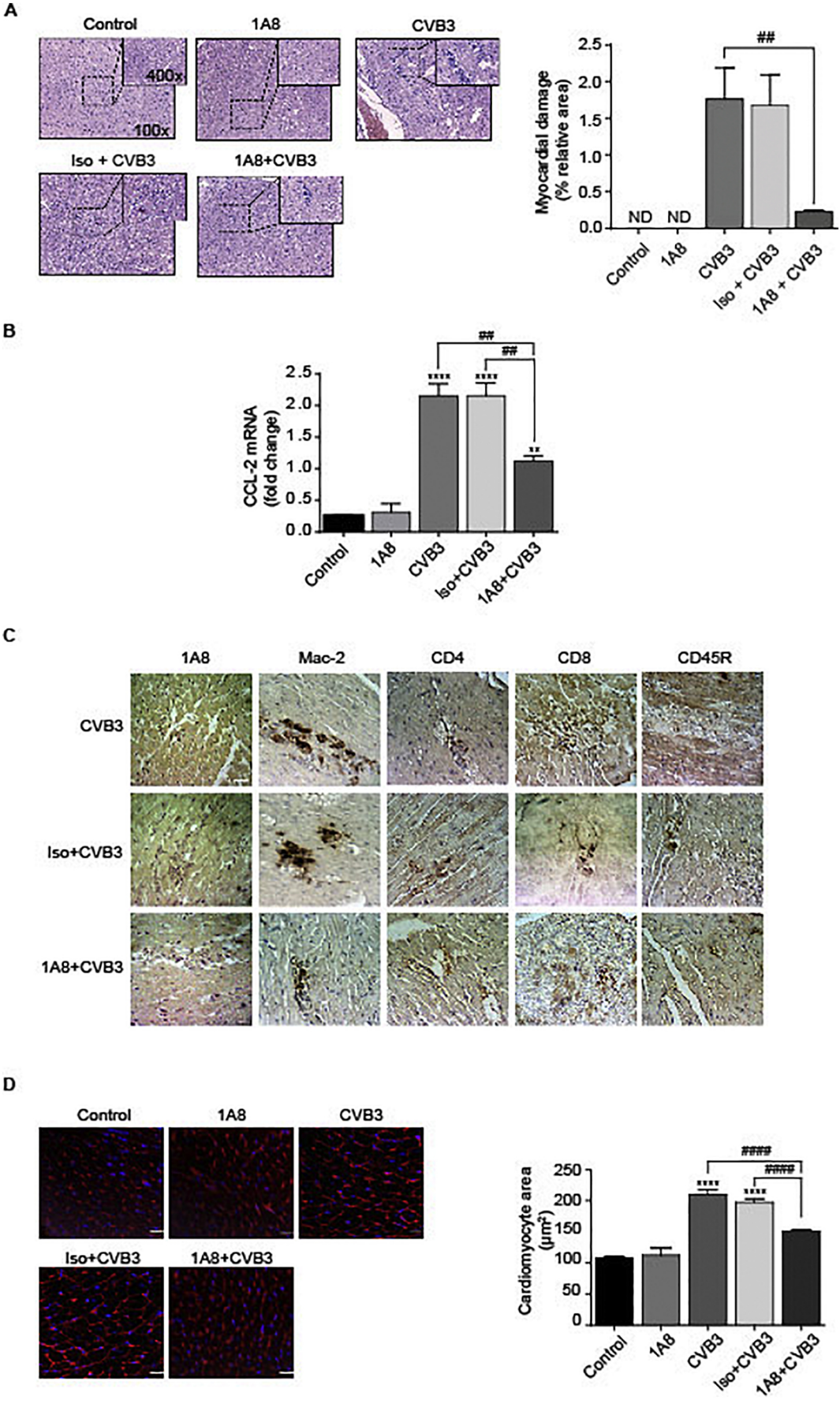
A
Control
1A8
CVB3
400x
100x
Iso + CVB3
1A8+CVB3
Myocardial damage (% relative area)
ND
ND
##
Control
1A8
CVB3
Iso + CVB3
1A8 + CVB3
B
CCL-2 mRNA (fold change)
##
##
****
****
**
Control
1A8
CVB3
Iso+CVB3
1A8+CVB3
C
1A8
Mac-2
CD4
CD8
CD45R
CVB3
Iso+CVB3
1A8+CVB3
D
Control
1A8
CVB3
Iso+CVB3
1A8+CVB3
Cardiomyocyte area (μm²)
####
####
****
****
Control
1A8
CVB3
Iso+CVB3
1A8+CVB3

Figure 9

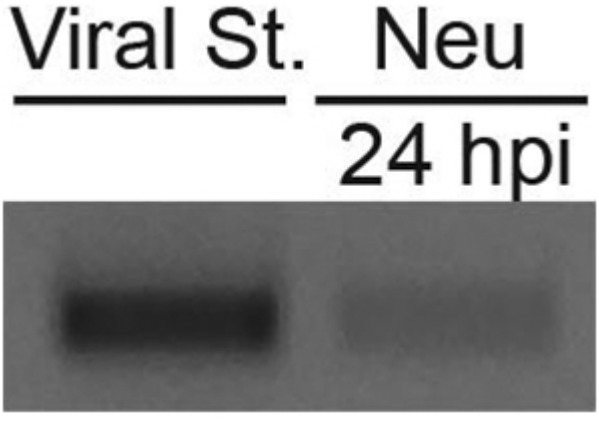

Figure 10

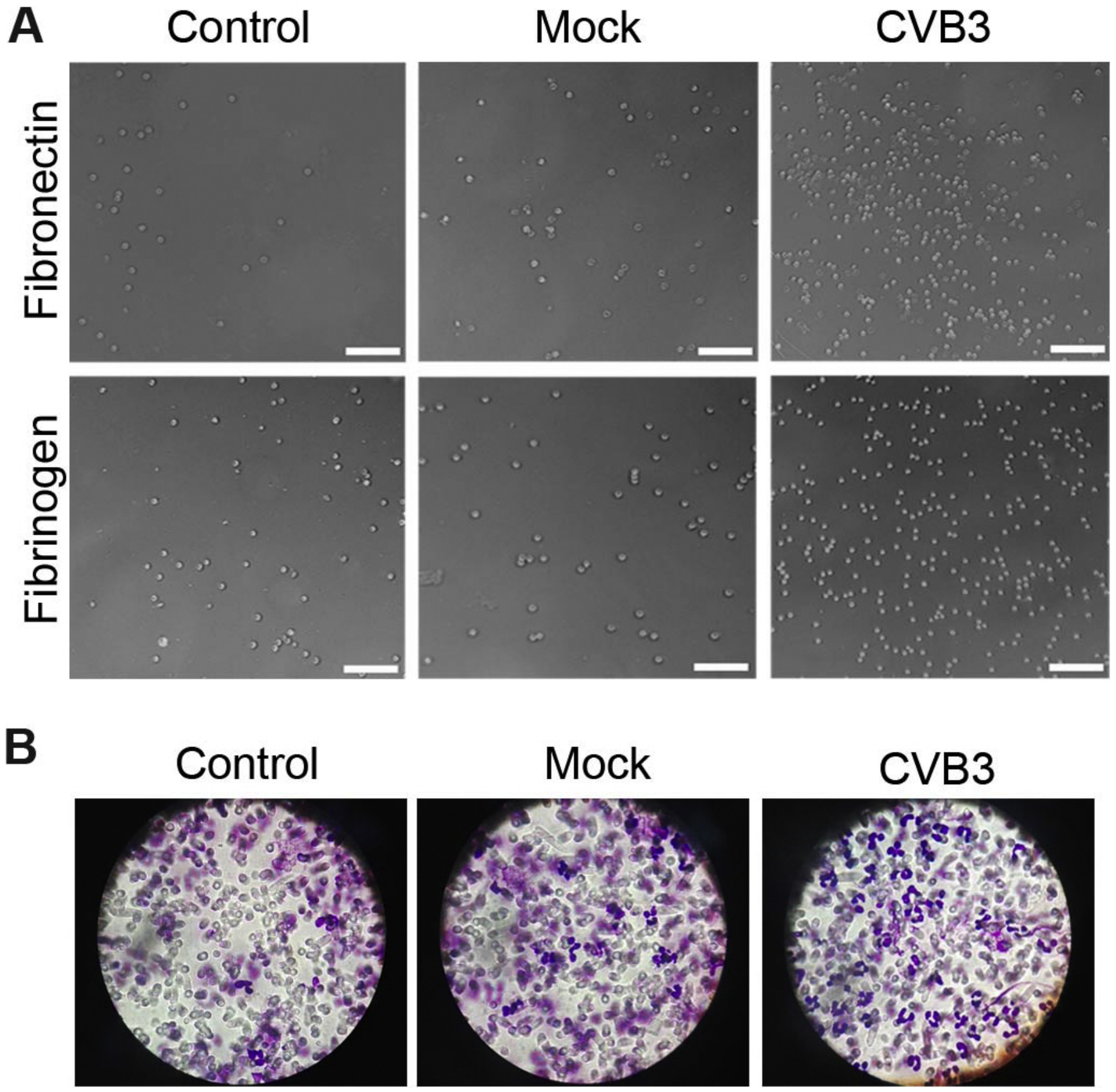
A
Control
Mock
CVB3
Fibronectin
Fibrinogen
B
Control
Mock
CVB3

Figure 11

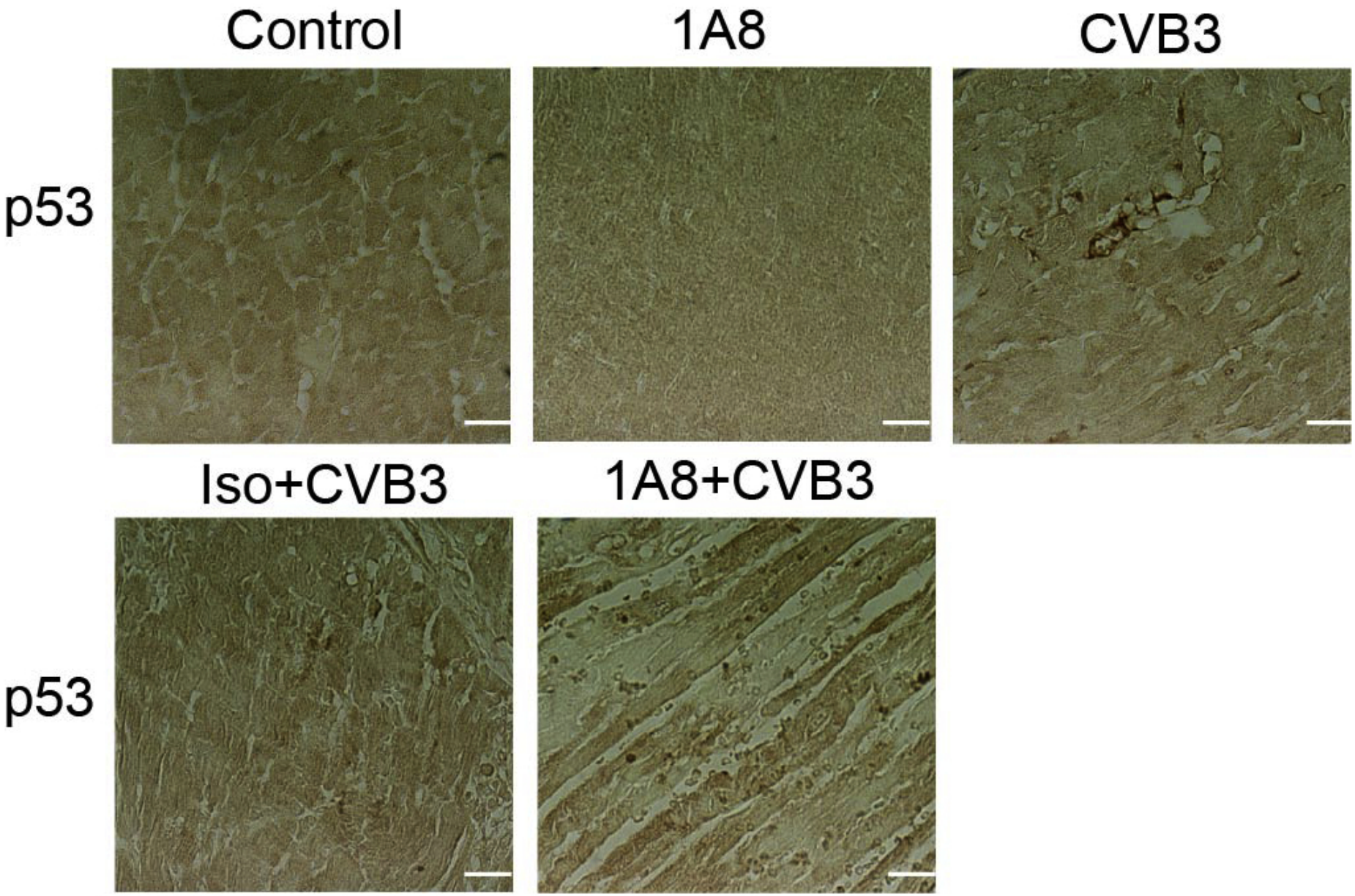

Figure 12